8-2019

Spiderworms: Using Silkworms as Hosts to Produce a Hybrid Silkworm-Spider Silk Fiber

Ana Laura Licon
Utah State University

SPIDERWORMS: USING SILKWORMS AS HOSTS TO PRODUCE A HYBRID SILKWORM-SPIDER SILK FIBER

by

Ana Laura Licon

A thesis submitted in partial fulfillment
of the requirements for the degree

of

MASTER OF SCIENCE

in

Biological Engineering

Approved:

_____	_____
Randy Lewis, Ph.D. Major Professor	Ron Sims, Ph.D. Committee Member
_____	_____
Jon Takemoto, Ph.D. Committee Member	Richard S. Inouye, Ph.D. Vice Provost for Graduate Studies

UTAH STATE UNIVERSITY
Logan, Utah

2019

ABSTRACT

SpiderWorms: Using Silkworms as Hosts to Produce a Hybrid

Silkworm-Spider Silk Fiber

by

Ana Laura Licon, Master of Science

Utah State University, 2019

Major Professor: Dr. Randy Lewis
Department: Biological Engineering

Spider silk has received significant attention due to its fascinating mechanical properties. The combination of sericulture, a millennia old practice, and modern advancements in genetic engineering has given rise to an innovative biomaterial inspired by nature. Due to the solitary and cannibalistic behavior of spiders, different hosts have been investigated for the mass production of synthetic spider silk and derived products. These hosts include genetically modified goats, E. coli, alfalfa, and silkworms. The synthetic spider silk proteins produced in most of these hosts are usually smaller than native size spider silk proteins and they are difficult to purify. Further, there is no established process to manufacture fibers from the synthetic proteins, and resulting products have low mechanical properties. Unlike the other hosts, silkworms are capable of producing large quantities of a fibrous product, in a manner mimetic to spiders, and there already exists an industry to process cocoons into threads and textiles for many applications. This project focuses on the creation of chimeric silkworm-spider silk fibers through the genetic modification of silkworms. Minor ampullate spider silk (MiSp)

genes were incorporated into the light chain (LC) region of the silkworm genome through CRISPR/Cas9 induced non-homologous end joining. A subset of these silkworms was cross-bred with other transgenic silkworms containing the same spider silk gene in the heavy chain (HC) region of the silkworm genome to create hybrid, dual-transgenic silkworms. Spider silk gene incorporation into the silkworm genome was verified using PCR. The transgenic silk samples showed increased mechanical properties compared to native silkworm fibers, with the strongest fibers approaching or surpassing the mechanical properties of native MiSp. Ultimately, genetic engineering opens the door to mass produce synthetic spider silk in an established organism and industry, and the results of this project demonstrate that the properties of silkworm silk can be predictably altered through this technology.

(94 pages)

PUBLIC ABSTRACT

SpiderWorms: Using Silkworms as Hosts to Produce a Hybrid Silkworm-Spider Silk Fiber

Ana Laura Licon

Spider silk has received significant attention due to its fascinating mechanical properties. Given the solitary and cannibalistic behavior of spiders, spider silk farming is impractical. Unlike spiders, silkworms are capable of producing large quantities of a fibrous product in a manner mimetic to spiders, and there already exists an industry to process cocoons into threads and textiles for many applications. The combination of silk farming (sericulture), a millennia old practice, and modern advancements in genetic engineering has given rise to an innovative biomaterial inspired by nature; transgenic silkworm silk.

This project focuses on the creation of chimeric silkworm-spider silk fibers through the genetic modification of silkworms. Advanced genetic engineering techniques were used to introduce the minor ampullate spider silk (MiSp) genes into the silkworm genome. A subset of these transgenic silkworms was cross-bred with other transgenic silkworms containing the same spider silk gene in a different section of the silkworm genome to create hybrid, dual-transgenic silkworms. The transgenic silk samples showed increased mechanical properties compared to native silkworm fibers, with the strongest fibers approaching or surpassing the mechanical properties of native spider silk. The transgenic silk retained the elasticity of the native silkworm silk and

gained the strength of the spider silk. Ultimately, genetic engineering opens the door to mass produce synthetic spider silk in an established organism and industry, and the results of this project demonstrate that the properties of silkworm silk can be predictably altered through this technology.

ACKNOWLEDGMENTS

I would like to thank my committee members, Drs. Randy Lewis, Ron Sims, and Jon Takemoto, for their continued support and guidance through this entire process, Dr. Xiaoli Zhang for teaching me about silkworms and their care, and Dr. Justin Jones and all my colleagues for their constant help and encouragement.

I would like to thank Dr. Yukio Saijoh, and Yuma Miyai from the department of Neurobiology and Anatomy at the University of Utah for allowing me to use their electroporator, and Drs. John Shervais, and Kelly Bradbury from the Geology department at Utah State University for allowing me to use their petrographic microscope.

Finally, I give special thanks to my family and loved ones for their endless encouragement, moral support, and patience as I worked on this project. My journey though this project would not have been possible without all of you.

Ana Laura Licon

CONTENTS

Page

LIST OF TABLES

LIST OF FIGURES

INTRODUCTION

Spider silk has fascinated people for centuries, and it has been used throughout history in a wide variety of applications. Ancient Greeks used spider silk for covering wounds; aborigines used it to make fishing line; and in WWII, spider silk was used as crosshairs in optical devices.[1] Many people have attempted to retrieve natural spider silk, whether by collecting webs and spiders' egg sacs or by inventing contraptions to immobilize spiders and harvest their silk, but these endeavors have generally failed due to the territorial and cannibalistic tendencies of spiders.[2] More recently two artists in Madagascar along with a team of 80 people collected spider silk from the *Nephila madagascariensis* spiders over five years to create a luxurious textile.[3] These examples, both artistic and practical, point towards the versatility of spider silk and its potential as a biomaterial for the future.[1–3]

For decades, researchers have been fascinated by spider silk's incredible mechanical properties, and spiders' silk spinning process. Spiders can produce up to six different types of silk and one glue.[4–7] Each silk is expressed and stored in a specific gland and serves a biological role for the spider. Figure 1 below depicts the seven spider silk glands, as well as their biological roles.[4] Despite originating in different glands, the types of spider silk share common features, they start as soluble protein solutions stably stored in glands at high concentrations, the proteins contain repetitive motifs with high amounts of serine, alanine, and glycine, and become insoluble fibers. It is the combination of these motifs that translate to the secondary and tertiary structures that give each type of spider silk its intriguing mechanical properties.[6–8]

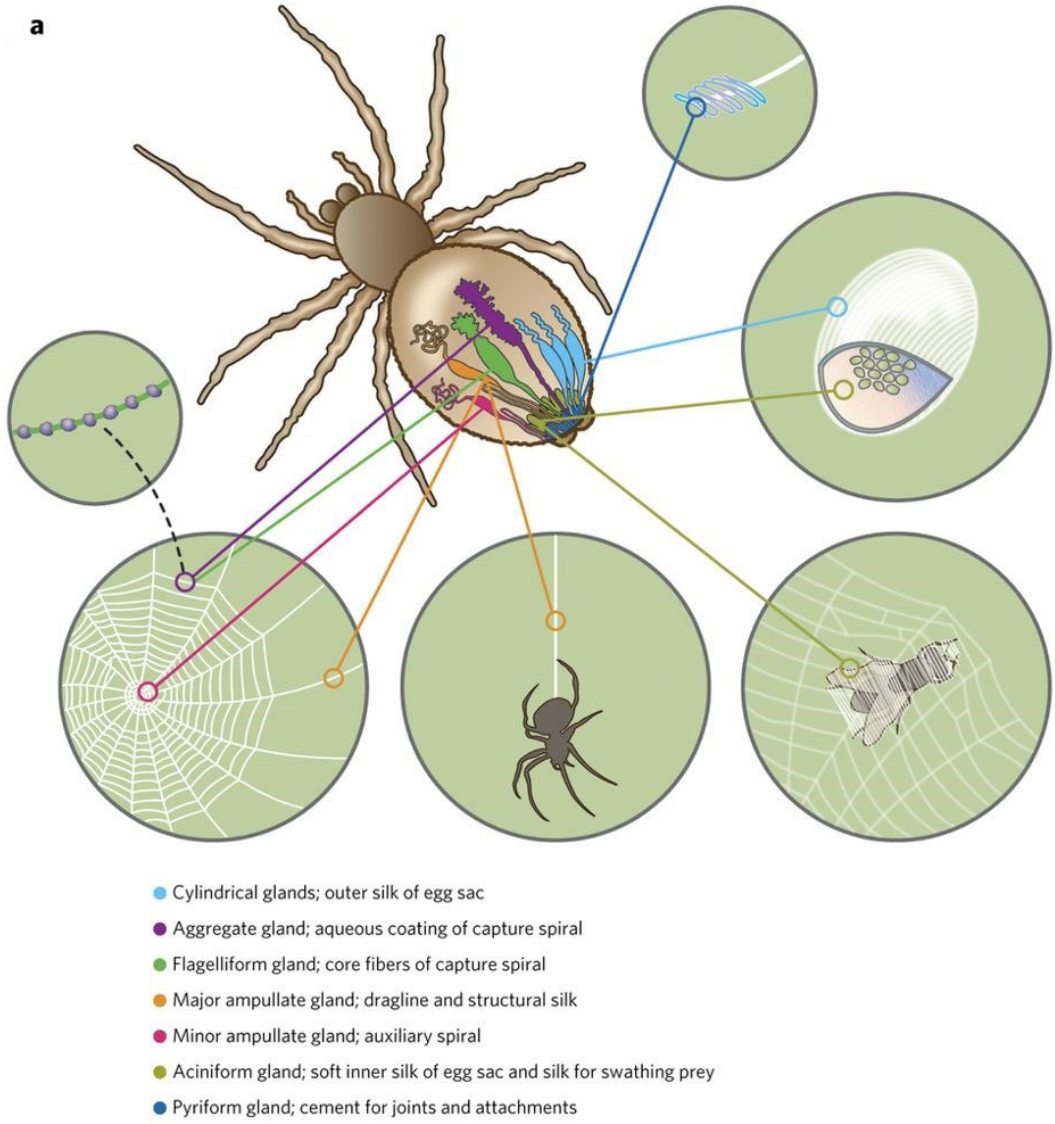

Figure 1. Depiction of the types of spider silk and originating silk glands.[4]

Major ampullate silk (MaSp), also known as dragline silk, is the most studied of the types of silk because it comes from the largest and most accessible of the spider silk glands, and it is also one of the strongest and toughest biological materials known.[9–11] Spiders use MaSp as the frame of the orb webs and as a safety line as they move around. Flagelliform silk is not as strong as MaSp but it is a highly elastic silk and is used as the

main capture spiral in an orb web.[12] The combination of strength and extensibility is what allows this fibrous biomaterial to absorb a large amount of energy with a very small amount of material. The flagelliform silk in the capture spiral of a web will absorb ~65% of the kinetic energy of an insect flying into it, converting it into heat rather than bouncing the insect from the web.[10] In addition, the aggregate spider silk serves as a sticky glue, further preventing the spider's prey from escaping the web.[13] Major ampullate spider silk proteins (MaSp1 and MaSp2) are large proteins (>250 kDa), which have highly repetitive regions rich in Gly and Ala.[7,14,15] Minor ampullate silk proteins (MiSps) are similar to MaSps; however, key differences in the protein sequence result in MiSp having a lower tensile strength and elasticity. The lower elasticity of MiSps is attributed, in part, to the lack of β-spirals which are formed by GPGXX motifs present in MaSp2.[16] The lower tensile strength is due to the decreased hydrophobic interactions in the β-sheet structures of the MiSps, caused by poly-GA motifs in MiSp replacing the longer poly-A motifs in MaSp. The glycines in the poly-GA β-sheets have lower binding energies than the poly-A β-sheets, resulting in the lower tensile strength.[15,17] MiSp also contains a highly conserved non-repetitive spacer region rich in serine and alanine.[18] The spacer region is very similar to the amorphous regions in silkworm silk, though the amorphous regions in the silkworms silk are composed of 30 amino acids and the MiSp spacer is composed of 137 amino acids.[6,19]

Despite having a wide range of mechanical properties with many potential applications, the main obstacle to spider silk product applications is the amount of synthetic protein material available for research. Large orb-weaving spiders are most commonly used to collect spider silk. Their large abdomens allow for easier research

into silk glands and silk production, but collecting spider silk fibers from even the largest spiders is laborious.[9] They are cannibalistic and territorial which makes them difficult to harvest for large-scale applications. It is also difficult to visually differentiate between the types of silk being collected from a web. Forced reeling of specific silk fibers results in uneven diameters and highly variable mechanical properties.[20] These obstacles impede the development of innovative spider silk products.

Since large amounts of spider silk protein are needed for research and product development, various hosts have been investigated to produce synthetic spider silk proteins. Both unicellular and multicellular organisms have been genetically modified to produce spider silk proteins; yet, heterologous hosts struggle to express these large, highly repetitive proteins to the full native size. As a result, many groups produce small (shortened, <120kDa generally) recombinant spider silk proteins (rSSps) are often difficult to purify.[9,11,21–23] Further, there is the need for artificial silk spinning methods which mimic the spider's spinning method.[24] This combination of small proteins and non-mimetic spinning methods results in fibers lacking the mechanical properties that make spider silk so unique.[14]

Under natural conditions, orb weaver spiders will attach the silk fiber to a surface and slowly move away to draw the silk out. Forced spinning can be used to get silk from spiders. However, in both natural and forced spinning, only a few tens of meters can be obtained from a single spider at a time and the rate at which the silk is drawn will have significant effects on the silk's mechanical properties.[8,25]

Artificial methods, such as wet spinning have also been used to spin rSSps into fibers. These methods extrude solubilized protein as thin fibers into a coagulation bath

which then get post treated to stretch the fibers and increase mechanical properties, but the vast majority of wet-spun fibers from even the most optimized methods still have lower mechanical properties than native spider silk.[8,14,24,26–29] There has been one study that successfully engineered *E.coli* to produce a native sized (284.9 kDa) spider silk protein which resulted in fibers with high mechanical properties approaching those of native spider silk , and also showed that fibers made from lower molecular weight proteins had lower mechanical properties. However, the amount of spider silk that the bacteria could produce decreased significantly with the increase in protein molecular weight.[14]

Industrial scale production of spider silk for materials applications has encountered many challenges, primarily the native-size production of rSSps, protein purification, and fiber spinning.[24] Silkworms are of particular interest in the large-scale production of spider silk because they naturally produce large amounts of silk fibers, and an industry exists for the large-scale production of silk.[30] Sericulture, the farming of silkworms for silk cultivation, is a centuries long practice that started in Asia possibly as early as the Neolithic era.[31] Given the correct environmental conditions, sericulture has served as the perfect industry to help growing rural economies in combination with agricultural practices.[32] Generally, silkworms feed on fresh mulberry leaves and grow in regions where the climate is favorable. The cocoons are then harvested for the silk before the pupae turn into moths and eat their way out of the cocoon[32]

Silk from the *Bombyx mori* species is the most commonly used in sericulture.[32] One silkworm cocoon is made of a dual fiber between 300 - 1200 m long.[33] The silkworm silk is composed of sericin and fibroin. The sericin acts like a glue to hold the

fibroin fibers together as the silkworm builds its cocoon. Fibroin is composed of three main proteins, the light chain (LC), the heavy chain (HC), and a glycoprotein (P25). The HC is a large protein (~350 kDa) and is connected to the LC (~26 kDa) with a disulfide bond. The P25 (~30 kDa) serves as a stabilizer of the six HC-LC units through non-covalent interactions, forming the fibroin elementary unit (Figure 2).[34] Like spider silk, the HC region of fibroin is composed of highly repetitive and hydrophobic regions rich in Gly, Ala, and Ser. These motifs, AGAGS, GAGAGY and GAGAGVGY, form beta sheet structures which are responsible for the mechanical strength of silk.[19,35–37] The LC of the fibroin silk is amorphous, with little or no crystalline regions and no repetitive motifs, giving the silk its elastic properties.[19] Combined with P25, the fibroin unit results in a fiber that is composed of 2/3 crystalline regions and 1/3 amorphous regions.[38,39]

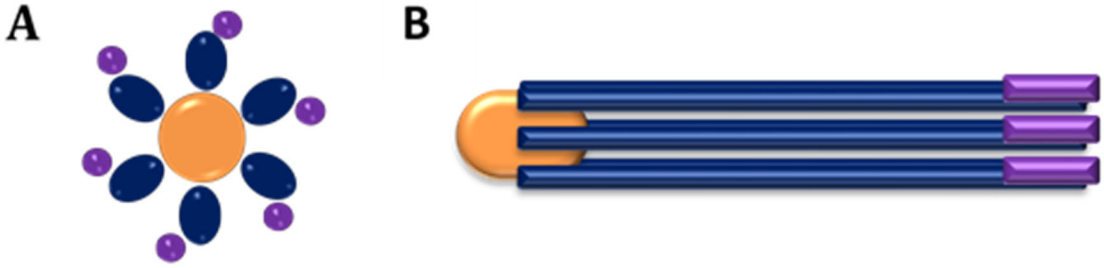

Figure 2. Illustration of orientation of fibroin unit components: P25-green, HC-blue, LC-purple. (A) cross sectional view of fibroin unit and (B) side view of fibroin unit.

Another advantage to using silkworms as hosts to produce spider silk is the similarities in silk spinning methods.[40,41] Silkworm silk glands originate from salivary glands and spider silk glands originate from ectodermal invaginations in their abdomen,

however despite different origins, the morphological and functional properties of the glands are very similar.[40,42] Figure 3 shows a side by side comparison of the silkworm silk gland (a,c), and a *Nephila clavipes* major ampullate gland(b, d).[40] Silkworm silk proteins are produced in the posterior silk gland (PSG) of silkworm silk gland. Spider silk proteins are produced in the tail of the major ampullate gland which is analogous to the PSG.[43,44] Silkworm silk proteins travel through the silkworm middle silk gland (MSG), funnel, and finally are transformed into a silk fiber in the anterior silk gland (ASG) before being spun through a specialized pore at the bottom of their mouth.[44] Spider silk proteins travel from the tail through the sac, funnel, and duct, and the fiber is spun through pores called spinnerets at the end of the spider's abdomen.[43] Both glands contain a pH gradient where the environment becomes more acidic as fiber formation begins.[45,46] The ASG and the duct have a constant decrease in diameter as the fiber is formed, to 50 μm and <10 μm respectively. The decreasing diameter as the silk passes through the tail of the glands induces shear force on the proteins which results in the proteins self-assembling and forming a fiber.[20,40,43,44]

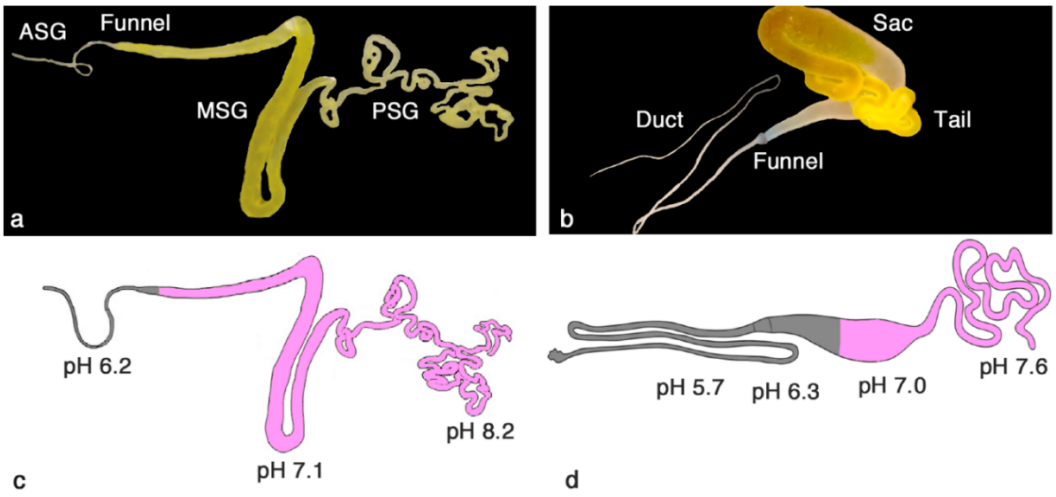

Figure 3. Macroscopic appearance of silkworm silk gland (a), and spider major ampullate gland (b) with pH gradients highlighted in purple for the silkworms silk gland (c) and spider major ampullate gland (d).[40]

Because of these similarities in silk gland structures as well as the fact that silkworms spin fibers, silkworms are ideal hosts for the large-scale production of spider silk fibers. Methods such as piggyBac vectors have been used to create genetically modified silkworms, which produce a chimeric silkworm/spider silk fiber.[47] More recently, CRISPR/Cas9 methods have also been used to create transgenic silkworms.

Prior to this study, three lines of transgenic silkworms have been made through CRISPR/Cas non-homologous end joining (NHEJ) using spider silk genes derived from the *Nephila clavipes*: MaSp1 gene cloned into the HC protein genomic locus (PGL), MaSp1 gene in the LC-PGL, and MiSp1 gene (without the spacer) in the HC-PGL. This project focuses on incorporating MiSp1 gene without the spacer into the light chain region of the silkworm genome (MiSp1 in the LC-PGL) using the same CRISPR/Cas9 system used to make previous transgenic silkworms.[48] Then, the transgenic silkworms will be cross-bred to make a hybrid line which has MiSp1 in both the HC-PGL and the

LC-PGL. The objectives of this project are summarized below:

- Use CRISPR/cas9 non-homologous end joining (NHEJ) to insert MiSp1 in the LC (light chain) region of the silkworm genome
- Cross breed transgenic lines (MiSp1-HC and MiSp1-LC) to create new hybrid fiber (MiSp1 HL)
- Confirm increased mechanical properties through tensile testing
- Validate the presence of MiSp1 gene in the silkworm genome and also its precise insertion in the LC by PCR
- Validate the presence of the MiSp1 protein in the silkworm fiber

Producing silk fibers with MiSp1 in the LC-PGL is significant for several reasons. First, silkworms are ideal hosts for large-scale spider silk fiber production, due to the ability to farm them in large quantities for their silk, and to the similarities with spiders in their silk spinning methods. Second, unlike other hosts silkworms can produce very large proteins, and therefore easily produce native size spider silk proteins, which translate to fibers with better mechanical properties. Third, cross-breeding transgenic silkworm with MiSp1 in the LC and MiSp1 in the HC will increase the amount of spider silk protein in the silkworm silk, potentially improving the mechanical properties. Finally, it is hypothesized that introducing the highly crystalline MiSp1 protein into the amorphous LC should increase the fraction of crystalline regions in the silk, resulting in a highly inelastic transgenic fiber with properties more like Kevlar.

The following chapters of this thesis describe the methods used for the genetic modification of the silkworms and testing of the transgenic silk; the results of the experiments; a discussion on the mechanical properties and the factors that influence the

mechanical properties of the transgenic fibers; the engineering significance of this project; and an overall conclusion.

MATERIALS AND METHODS

DNA Plasmids Construction

To start the process of silkworm genome modification, DNA expression plasmids were constructed through a combination of PCR, restriction enzyme digestions, and ligations. These plasmids consist of gene inserts which were added into the standard cloning vector pBluescript SK + II. The gene inserts consist of N and C terminus domains (NTD and CTD), an enhanced green fluorescent (eGFP) reporter gene, and the MiSp1 64/48 genes. Figure 4 depicts the order of the DNA inserts in the cloning vectors and Table 1 shows the gene sequences with the restriction enzyme cut sites used in each ligation.

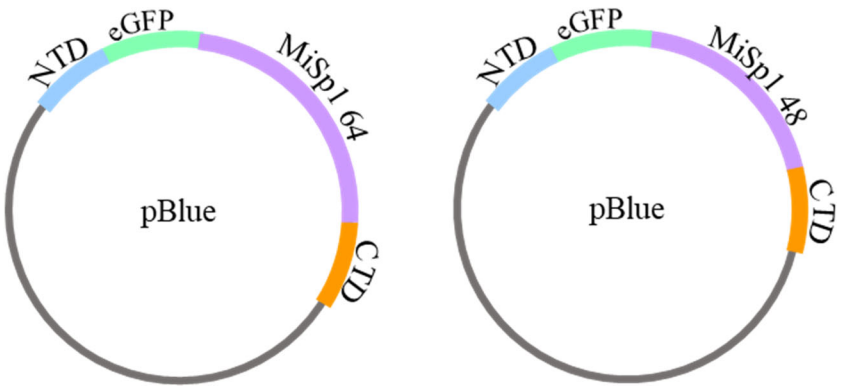

Figure 4. Depiction of DNA expression plasmids, showing the order of the DNA inserts in the pBluescript SK + II vector.

Table 1. Gene sequences used in this project, with restriction enzyme cut sites.

Gene	Sequence
N terminus (NTD) with a KpnI restriction enzyme cut site at the 5' end and a SalI restriction enzyme cut site at the 3' end	GGTACCCCGGTTGCTCAAGTGTTCCACCAATCAGCTGGATCAATCACAGACGTAAGT TACTTTAAATTACCCAGGGTCTTTATGTAATTTTGTTATTAGTAATGATTGGACAAAT GAGCTTATCGCCGATTCGTCACGATCACTCGTCACTGATGTCACAAAGGTCACAAAG TGAACGTGTTTTGGAGTTGATAGATATAGAAACTCCTTATCAACAAAAAAAAAAAAT ACATAGACAGCAGTGACAATAGGTGTCTAAAAAAAAAGTGAAATAATGTCTGTCGG TTCGAGAAGTAAAACAAAATAACAAAACTGTGATTTTGATTAAAAAAAATCTAAAG CATCCACGTATTTAATTCTAATTTATAAAAGTGTGTTAGTATGTTATTTCGTAACTGC CTGCACTCTGTGATTTAAAGATTGGACTTTGCTACCAAGAACTTTAAATTATATCTAC GCGACCATCACTATGAGACTTAAGCTGAAATTATTTCTTTCAAAACACGCTTCATAG ATTTAAAGCTGCCCTTCAATCCAGACATATAAGAGCTACGAATCAGACTTAGGCCAG CAAGGTGTCCATCTTGTTTTTACCACCTAAATTGGGACTACTATATATTAATTCACGT TTTTAATTATCCACAGCTCCTGAGAGGCGTTGGCAACGGTAATGACGTCGAC
C terminus (CTD) with a BamHI restriction enzyme cut site at the 5' end and an extra T nucleotide to keep sequences in frame, and a SalI restriction enzyme cut site at the 3' end	GGATCCTGCGACCGGCTTAGTTGCTAATGCTCAAAGATATATTGCACAAGCAGCCAG CCAGGTTCACGTCTAAATAAGAACTGTAAATAATGTATATATATAATTATATAAAAG ATATATATAACCATATACAAACATATATATCATTATAAGACAATCTACCTATATAAA AACAGACTAAAATTAATAATTATGTATACTTTAATTGTGTTTAGGACATTTTATGCAA ATTGTGTTTGCGTTAGGATTTTTTTTGGAAGTTTTTTAGATTATTTATGAATATATAAA TAAATATACGTTAATATAATATATATTATATAAATCAACGACACGGCTTTTCATTTTG GTGATGATCAATCTTATTGTTCTTCTAATTGATTTTTTTGTACAATAAAGATGTATCC AGTTTTCCAGATAAAGAATTTAGTTTGTTATTTCTGGCCCCATTAAAATAAGTACGGT ATTCGACAATACCACATAGTATATACCCAAAGACGGTGGATTGGACAGTGGGTACGAGCTC
eGFP with a SalI restriction enzyme cut site at the 5' end and a HindIII restriction enzyme cut site at the 3' end	GTCGACGTGAGCAAGGGCGAGGAGCTGTTCACCGGGGTGGTGCCCATCCTGGTCGA GCTGGACGGCGACGTAAACGGCCACAAGTTCAGCGTGTCCGGCGAGGGCGAGGGCG ATGCCACCTACGGCAAGCTGACCCTGAAGTTCATCTGCACCACCGGCAAGCTGCCCG TGCCCTGGCCCACCCTCGTGACCACCCTGACCTACGGCGTGCAGTGCTTCAGCCGCT ACCCCGACCACATGAAGCAGCACGACTTCTTCAAGTCCGCCATGCCCGAAGGCTACG TCCAGGAGCGCACCATCTTCTTCAAGGACGACGGCAACTACAAGACCCGCGCCGAG GTGAAGTTCGAGGGCGACACCCTGGTGAACCGCATCGAGCTGAAGGGCATCGACTT CAAGGAGGACGGCAACATCCTGGGGCACAAGCTGGAGTACAACTACAACAGCCACA ACGTCTATATCATGGCCGACAAGCAGAAGAACGGCATCAAGGTGAACTTCAAGATC CGCCACAACATCGAGGACGGCAGCGTGCAGCTCGCCGACCACTACCAGCAGAACAC CCCCATCGGCGACGGCCCCGTGCTGCTGCCCGACAACCACTACCTGAGCACCCAGTC CGCCCTGAGCAAAGACCCCAACGAGAAGCGCGATCACATGGTCCTGCTGGAGTTCG TGACCGCCGCCGGGATCACTCTCGGCATGGACGAGCTGTACAAGAAGCTT
MiSp1 8 repeat unit with HindIII, and AgeI restriction enzyme cut sites a the 5' end and a BspEI and BamHI restriction enzyme cut sites at the 3' end.	AAGCTTCATATGACCGGTGGTGCCGGTGGTTATGGTCGTGGTGCTGGTGCGGGTGCC GGTGCAGCAGCTGGTGCCGGTGCTGGCGCAGGCGGTTATGGTGGTCAGGGTGGCTA CGGTGCCGGTGCCGGTGCTGGTGCCGCAGCCGCAGCGGGTGCGGGTGCAGGCGGTG CTGGCGGTTATGGCAGAGGTGCTGGGGCTGGTGCAGGCGCTGCAGCCGGTGCGGGT GCTGGTGCGGGTGGATATGGTGGCCAGGGTGGTTATGGCGCTGGCGCAGGGGCAGG CGCAGCAGCAGCAGCTGGGGCAGGCGCAGGCGGTGCCGGTGGCTATGGACGCGGAG CCGGTGCCGGTGCAGGGGCAGCAGCGGGTGCTGGTGCCGGTGCAGGGGGTTATGGT GGCCAAGGCGGATATGGTGCGGGTGCAGGCGCTGGTGCAGCAGCAGCCGCTGGTGC CGGTGCCGGTGGTGCGGGTGGCTACGGAAGAGGTGCGGGTGCCGGTGCCGGTGCTG CAGCGGGTGCGGGTGCGGGTGCCGGTGGTTATGGCGGTCAGGGTGGGTATGGTGCG GGTGCTGGTGCAGGCGCAGCTGCAGCCGCTGGTGCTGGTGCAGGCGGAGCCGGTGG ATATGGCCGAGGTGCTGGCGCAGGCGCTGGCGCTGCTGCTGGTGCCGGTGCGGGTGC TGGGGGATACGGTGGTCAAGGGGGTTATGGTGCGGGTGCCGGTGCGGGTGCAGCCG CAGCAGCTGGTGCGGGTGCGGGTGGTGCAGGGGGATATGGCCGTGGTGCCGGTGCT GGTGCGGGTGCTGCAGCCGGTGCTGGGGCAGGGGCTGGCGGTTATGGGGGTCAAGG CGGTTATGGCGCTGGTGCTGGTGCTGGGGCTGCCGCAGCAGCCGGTGCTGGTGCTGG CGGTGCGGGTGGTTACGGTCGGGGAGCTGGCGCTGGTGCTGGCGCAGCAGCGGGTG CCGGTGCTGGTGCCGGTGGCTACGGTGGACAAGGTGGCTATGGTGCCGGTGCAGGC GCAGGGGCTGCAGCCGCAGCCGGTGCCGGTGCCGGTGGCGCTGGGGGTTATGGTCG CGGAGCGGGTGCAGGCGCAGGCGCAGCCGCTGGCGCTGGTGCGGGTGCTGGCGGTT ATGGTGGACAAGGGGGTTATGGGGCTGGTGCTGGCGCAGGGGCAGCTGCTGCAGCG GGTGCTGGCGCTTCCGGAGGGGATCC

MiSp1 48 and 64

Plasmids (pMK) containing 16 and 32 repeats of the minor ampullate spider silk 1 (MiSp1) gene were obtained from a previous project.[48] A sequence of 8 repeats of the MiSp1 gene can be seen in Table 1. To make the MiSp1 48 gene, first the vector containing the MiSp1 16 gene was cut out from the plasmid with a sequential restriction enzyme digestion using AgeI-HF® first and then BspEI. A sequential digestion was necessary instead of a regular double digestion since AgeI-HF® and BspEI do not exhibit high activity in the same buffers. AgeI-HF® only exhibits 100% activity in 1.1 and CutSmart® Buffer, but BspEI only exhibits 100% activity in the 3.1 buffer

For the sequential digestion, a 50 µl digestion was first set up using 1µg of the MiSp1 16 in the pMK vector, 1 µl of the AgeI-HF® restriction enzyme, 5 µl of the CutSmart® Buffer, 40 µl of ddH_2O, and was incubated for 1 hour at 37 °C. Then 5.6 µl of 1 M NaCl were added to the digestion to approximate the salt concentration of the 3.1 buffer, and 1 µl of the BspEI restriction enzyme was added before incubating the digestion for 1 more hour at 37 °C. This sequential digestion resulted in a MiSp1 16 segment of about 2.4 kb with CCGG overhangs at each end. At the same time the MiSp1 32 in the pMK vector was linearized with a single BspEI enzyme digestion, using 1µg of the MiSp1 32 in the pMK vector, 1 µl of the BspEI restriction enzyme, 5 µl of the CutSmart® Buffer, 40 µl of ddH_2O, and was incubated for 1 hour at 37 °C. This digestion resulted in an approximately 7.1 kb DNA segment, also with CCGG overhangs.

Following the digestions, the MiSp1 16 sample was separated from the vector via gel electrophoresis using a 1% agarose gel with Midori Green DNA Stain run at 100

V for 30 minutes. The DNA bands were observed under UV light. The MiSp1 16 band was cut from the gel, purified using a Promega Wizard® SV Gel and PCR Clean-Up System, and the linearized MiSp1 32 vector was purified with the same Promega Wizard® SV Gel and PCR Clean-Up System. The linearized MiSp1 32 vector and isolated MiSp1 16 segment gene were ligated together to form a plasmid containing 48 repeats of the MiSp1 gene, approximately 9.5 kb long. The ligation was conducted using a NEB T4 DNA ligase kit, with a 6:1 molar ratio of MiSp1 16 insert to MiSp1 32 with pMK vector in a volume of 20 µl, incubated overnight at 4 °C. The ligation between the BspEI and AgeI overhangs resulted in a TCCGGT sequence, creating a seamless connection without a restriction enzyme site re-cleavable by either enzyme. The MiSp1 64 gene was ligated in the same way, except both the single and sequential restriction enzyme digestions were done on MiSp1 32.

After each ligation, the solutions were transformed into TOP10 chemically competent cells. Two microcentrifuge tubes of competent cells, stored at -80 °C, were thawed on ice for 15 minutes. Once thawed 3 µl of ligation solution were added to the cells, one microcentrifuge tube for the MiSp1 48 ligation and one for the MiSp1 64 ligation. The cells with the ligation solution were incubated on ice for 30 minutes, heat shocked at 42 °C for 30 seconds, and incubated on ice again for 2 minutes. 250 µl of S.O.C. medium from Invitrogen were added to the cells, and the tubes were incubated in a shaker at 37 °C for 1 hour. After incubation, 200 µl of the cells were plated onto LB agar plates with kanamycin and incubated at 37 °C overnight to allow cell colonies to grow.

Individual colonies (10-12) from each plate were picked, and each colony was

used to inoculate 5 ml of LB medium with kanamycin in culture tubes. The tubes with inoculated medium were incubated overnight in a shaker at 37 °C to allow the cells to grow. Once the cells grew in the media the MiSp1 48 and MiSp1 64 pMK plasmids were purified from the cells using a High-Speed Plasmid Mini Kit from IBI Scientific and eluted into 50 µl of ddH_2O.

The purified plasmids from each tube were double digested using BamHI-HF® and HindIII-HF® to check for the correct ligation. Digestion reactions were each set up using 0.5 µl of each restriction enzyme, 2 µl of eluted plasmid, 2 µl of CutSmart® Buffer, and 15 µl of ddH_2O. Digestions were incubated at 37 °C for 1 hour. The digested plasmids were then separated through agarose gel electrophoresis using a 1% agarose gel run at 100 V for 30 minutes. The gel was soaked in a 1 µg/ml solution of Ethidium bromide for 30 minutes and de-stained in water for the same amount of time, making the DNA bands visible under UV light. By digesting the plasmid with BamHI and HindIII the complete MiSp1 48 and MiSp1 64 repeats could be separated from the pMK plasmid, and the ligation could be verified by the band sizes. Successful ligations resulted in bands approximately 7.1 kb long for MiSp1 48, and approximately 9.4 kb long for MiSp1 64 with the pMK bands around 2.4 kb long.

NTD, eGFP, and CTD

Since the NTD and CTD genes are much smaller than the MiSp1 repeats they could be easily amplified through polymerase chain reactions. A PCR was conducted for each gene from template plasmids using a Phusion® High-Fidelity PCR Master Mix with HF Buffer from NEB. Two reaction solutions were set up in 0.2 ml flat cap tubes,

one for the NTD and one for the CTD. Each solution had 7 µl of ddH_2O, 1 µl of the corresponding reverse primer, 1 µl of the corresponding forward primer, 1 µl of the DNA template, and 10 µl of the Phusion® High-Fidelity PCR Master Mix. The DNA template consisted of a pMK plasmid which contained the NTD and the CTD sequences. The reactions were set up for 35 cycles with a 10 second denaturation time at 98 °C, a 30 second annealing time at 60 °C, and a 20 second extension time at 72 °C, as well as an overall initial 30 second denaturation time at 98 °C and a final 5 minute extension time at 72 °C. PCR primers can be seen in the Table 2 below.

Table 2. PCR primer sequences used for PCR of NTD and CTD.

DNA Sequence	Primers	
N terminus (NTD)	**Forward**	5'-GGTACCCCGGTTGCTCAAGTGTTCCACC-3'
	Reverse	5'-GTCGACGTCATTACCGTTGCCAACGCCTC-3'
C terminus (CTD)	**Forward**	5'-GGATCCTGCGACCGGCTTAGTTGCTAAT-3'
	Reverse	5'-GAGCTCGTACCCACTGTCCAATCCACCG-3'

Each PCR product was separated from the template plasmids though gel electrophoresis and purified with a Promega Wizard® SV Gel and PCR Clean-Up System. Following purification, the PCR products and a pBluescript SK + II plasmid which already contained the eGFP gene (pBlue+eGFP), were digested with restriction enzymes to create overhangs for ligations. Both the NTD gene and the pBlue+eGFP plasmid were digested with SalI and KpnI restriction enzymes, incubated for 1 hour at 37 °, and purified with a Promega Wizard® SV Gel and PCR Clean-Up System.

The ligation was conducted using an NEB T4 DNA ligase kit, with a 6:1 molar

ratio of NTD insert to pBlue+eGFP vector in a volume of 20 µl, incubated overnight at 16°C. 2 µl of the ligation reaction were transformed into TOP10 competent cells following the same steps as with the MiSp1 48 and MiSp1 64 ligations, except the cells were plated on LB agar plates with ampicillin because the pBluescript SK + II plasmid has an ampicillin resistance gene. Of the colonies that grew on the plate, 6-12 were selected and each used to inoculate a culture tube with 5 ml of LB media with ampicillin and incubated at 37 °C overnight. The DNA plasmids were purified from the cells via minipreps using a High-Speed Plasmid Mini Kit from IBI Scientific and eluted into 50 µl of ddH_2O. The plasmids from each miniprep were then digested using 15 µl of ddH_2O, 2 µl of DNA, 0.5 µl of each restriction enzyme (SalI and KpnI), and 2 µl of the CutSmart® Buffer, incubated at 37 °C for 1 hour. A 1% agarose gel electrophoresis was conducted at 100V for 25 minutes to confirm if the ligation was successful, by getting DNA bands of the correct sizes. The correct band sizes for the NTD gene were approximately 700 bp, and 3.7 kb for the pBlue+eGFP vector. The bands were visualized by soaking the gel in a 1 µg/ml solution of Ethidium bromide for 30 minutes and de-stained in water for the same amount of time, and then placing the gel under UV light.

The CTD gene was ligated into the vector following the NTD. The CTD gene and the plasmid with the successful NTD ligation were digested with BamHI and SacI. The same ligation, transformation and miniprep processes were followed as with the NTD ligation but using the corresponding BamHI and SacI restriction enzymes. The correct band sizes were about 500 bp for the CTD insert and 4.3 kb for the pBlue+NTD +eGFP vector.

The process to ligate the MiSp1 48 and MiSp1 64 genes into the vector was similar. The expression plasmid pBlue+NTD +eGFP +CTD and the MiSp1 48 and MiSp1 64 plasmids were each digested using 5 µl of DNA, 38 µl of ddH_2O, 1 µl each of BamHI and HindIII, and 5 µl of the CutSmart® Buffer, incubated at 37 °C for 1 hour. A 1% agarose gel electrophoresis was run at 100 V for 35 minutes to separate the digested plasmid bands. The bands were visualized by soaking the gel in a 1 µg/ml solution of Ethidium bromide for 30 minutes and de-stained in water for the same amount of time, and then placing the gel under UV light. The corresponding band sizes were 7.1 kb for the MiSp1 48, 9.4 kb for the MiSp1 64 and 4.9 kb for the Blue+CTD+eGFP+NTD. These bands were cut from the gel purified using a Promega Wizard® SV Gel and PCR Clean-Up System. Since the MiSp1 48 and MiSp1 64 genes were much larger than the expression vector, the insert:vector ratio was reversed, with the MiSp1 genes acting as the vector, and the expression plasmid as the insert. Two 20 µl ligations were conducted, one for the MiSp1 48 expression plasmid and one for the MiSp1 64 expression plasmid, using an NEB T4 DNA ligase kit, with a 3:1 molar ratio of Blue+NTD+eGFP+CTD to MiSp1 and 0.2 µl of DMSO.

Electroporation and CRISPR/Cas9

The completed MiSp1 48 and MiSp1 64 expression plasmids were added into the silkworm eggs through a process called electroporation. Electroporation requires fresh silkworm eggs, so non-transgenic silkworms were raised to cocoons, allowed to hatch,

and paired off to mate. More details on growing silkworms are in the sericulture section. The moths were separated after mating for 3-5 hours and the females were placed on circle cutouts of construction paper. 300-500 freshly laid silkworm eggs (laid within 2 hours) were collected in a petri dish for each group. The eggs were soaked with reduced pressure in an electroporation buffer on ice in a vacuum chamber for one hour. To make the electroporation buffer the following were combined: 385 ul of water, 250 ul of 2% PVP, 15 ul of 10% Tween 20, 50 ul of 0.1 M spermidine, 40 ul of gRNA 5 plasmid (1 ug/ul), 40 ul of gRNA 6 plasmid (1 ug/ul), 80 of the corresponding MiSp1 48 or MiSp1 64 expression plasmid (1 ug/ul), 40 ul of Cas9 plasmid (1 ug/ul), and 100 ul of 2.5 M $CaCl_2$. The gRNA and Cas9 plasmids were obtained from a previous project in the lab[48]. After soaking in the electroporation buffer, the eggs were transferred into a 2 cm wide electroporation chamber and covered with 1 ml of the electroporation buffer. The electroporation chamber was connected to a CUY21 electroporation instrument and the eggs were electroporated at a specific voltage, current, and resistance, allowing the DNA plasmids through the egg membrane and into the developing silkworm cells. Typical electroporation conditions were: 15 V, 50 ms pulse, 75 ms interval, repeated 15 times.

Inside the egg cells the gRNA and Cas9 DNA plasmids were transcribed and translated into the proper machinery for CRISPR/Cas9 induced non-homologous end joining (NHEJ). The gRNAs signaled the correct spot in the light chain (LC) region of the silkworm genomes, where the Cas9 proteins introduced a doubled stranded cut, and linearized the spider silk plasmids. The spider silk genes could then repair the double stranded cut and be incorporated in to the silkworm genome through NHEJ. The repair processes of DNA double stranded cuts are depicted in Figure 5 below[49]. NHEJ was

chosen for this project because it is more efficient than homologous directed repair (HDR), though less precise, and does not require large homologous arms for insertion. Although HDR is more precise than NHEJ, it is much less effective due to the large size of the desired insertion, and there was no concern of the DNA inserts being out of frame since they have their own start and stop codons.

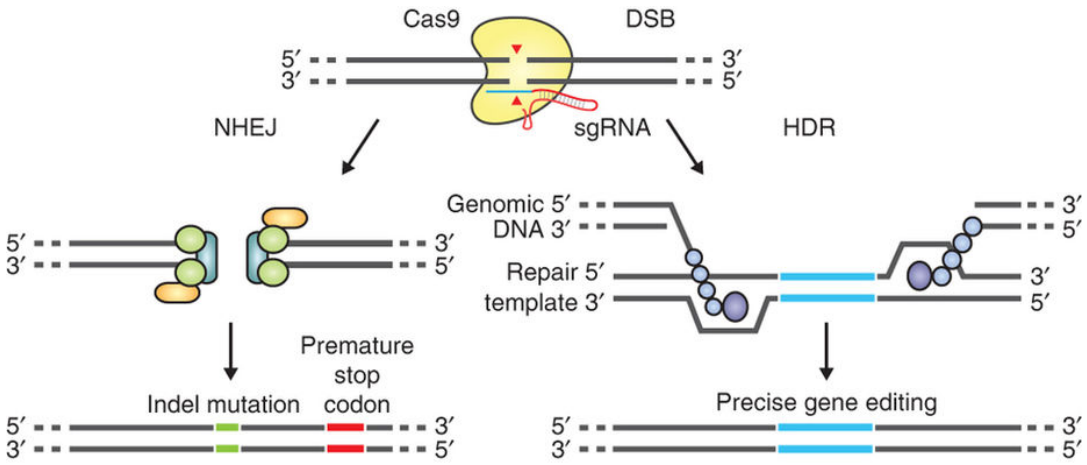

Figure 5. Depiction showing the difference between non-homologous end joining (NHEJ) vs homologous directed repair (HDR).[49]

Finally, the transgenic line of silkworms made in this project (MiSp1 in the LC) were cross bred to a transgenic line from a preceding project (MiSp1 in the HC) to make a hybrid transgenic silkworm line with MiSp1 in both the heavy chain and the light chain. The MiSp1 in the LC and the hybrid MiSp1 in the HC and LC lines of transgenic silkworms were grown in the same environment, and their silk was treated and tested under the same conditions.

Sericulture

Sericulture is the cultivation of silkworms for their silk. The transgenic silkworms created were kept in controlled conditions, in an effort to keep them healthy and ensure good quality silk. The conditions for the young worms, between the 1st and 3rd larval stage, were maintained between 26-28 °C with 70-80% relative humidity (RH), and for the silkworms in the 4th and 5th larval stages the conditions were kept between 25-27 °C and 60-70% RH.

The silkworms are raised in containers lined with plastic wrap to help waste clean-up. As the worms grow they are moved to larger containers lined with a mesh to separate the waste from the worms and food. All containers were cleaned and autoclaved between each use. The cleaning step was especially important to help prevent the spread of infections, which occur often and result in high silkworm death rates. The silkworm room, and everything taken into the room was also cleaned periodically with bleach, and any person in the silkworm room was also required to wear disposable gloves, face mask, lab coat, and booties to help prevent contamination from outside sources.

The whole silkworm lifecycle from egg to moth takes about two months, though the eggs can go into a dormancy state called the diapause period which lasts another two months. To circumvent the diapause period, freshly laid eggs are treated in a 1:1.6 solution of hydrochloric acid and water for 5 minutes at 46 °C. If the eggs have changed color from yellow or pink to a dark grey, then the diapause period has been entered and the eggs must be stored for 60 days before treating them the HCl solution.

After the acid treatment the eggs will hatch in 10-14 days. The worms are about

3 mm long when they hatch and shed their skin four times, marking the five larval stages. At their largest silkworms grew to about 6 cm, before shrinking slightly to spin cocoons and become pupae. The silkworms were grown to the 5th larval stage, when they were ready to spin cocoons. They were placed in 1-1.5 in diameter paper rolls in groups of three to allow for enough space for the worms to form individual cocoons, rather than large cocoons composed of silk from two or even three worms together, and to make sure the cocoons were not deformed or ruined by their surroundings. Inside the cocoons, the pupae will metamorphose into silk moths. Typically, the moths eat their way out of the cocoons and will live for a few days, only to mate and lay eggs before dying and leaving their eggs to hatch and start the silkworm life cycle once again. For the purpose of this project, some of the cocoons were collected (before the moths hatch) for silk harvesting while others were allowed to hatch to breed the next generation of silkworms. Non-transgenic silkworms are raised at the same time as the transgenic groups and served as a comparison group. Once the moths had finished mating and laying eggs, some of them were collected, labeled, and frozen at -20 °C for later genomic extractions.

The sericin that holds to cocoon together must be removed through a process called degumming which involves soaking the cocoons in a solution of sodium carbonate and SDS. Once the initial layers of sericin are removed the silk can be unwound onto spools of up to 33 ply threads. This unwinding process is used to gather large amounts of silk. Otherwise, small pieces of the cocoons can be completely degummed, and the mats of silk are used to collect un-stretched silk fibers for mechanical testing.

Spider Silk Reeling

Nephila clavipes spiders were ordered and kept in the lab under warm and humid conditions. To collect native spider silk, individual spiders were briefly exposed to carbon dioxide gas for easier handling. The spider was carefully immobilized on a petri dish with the spinnerets facing up, and the petri dish was placed under a ThermoFisher Stereomaster microscope. The microscope was then used to identify the spinnerets, tweezers were used to slowly pull the silk out and the silk was attached to a dark spool for easier visualization and reeled at a rate of 1 m/min. After 30-40 meters of silk were collected, the spider was placed back into its container and treated to a nice juicy cricket.

The beginning and ends of the reeled silk were marked clearly, to avoid and problems when removing the silk from the spool. Silk was gently removed from the spool to avoid overstretching and carded in the same manner as the silkworm silk to prepare it for mechanical testing.

Mechanical Testing

The transgenic and control cocoons were collected once the worms had finished spinning silk and transformed into pupae. The cocoons were sorted based on green fluorescence under UV light, due to the presence of the eGFP reporter protein inserted with the spider silk. Brighter cocoons indicate a higher presence of spider silk in the transgenic fiber.

Typically, the silk moths hatch and chew their way out of the cocoons. However, if the silk is to be harvested, the cocoons must remain intact, so the long silk fiber is not broken, and the pupae cannot be removed from the cocoon. At the lab scale it is not usually necessary to harvest the silk from the whole cocoon. The selected cocoons are cut open using a small blade and the pupae are removed. These pupae were allowed to hatch and breed for the next generation of silkworms. Approximately 1/3 of each cocoon was cut off, to be prepared for degumming (sericin removal).

A degumming solution was prepared with 0.25% w/v Na_2CO_3 in water. Each cocoon segment was placed in a small glass bottle (100 ml) and filled with ~80 ml of the degumming solution. The bottles were kept in a water bath at 85°C and mixed constantly until the sericin was dissolved, and the cocoon fibers separated into a cloud-like shape. The silk "clouds" were collected from the bottles and individually rinsed in water before air drying on a flat surface into a silk mat. Individual fiber segments were selected from each mat without pulling too much on the fibers, to preserve the fibers mechanical properties for tensile testing. Native MiSp from the *Nephila clavipes* spider was also collected and prepared for mechanical testing.

Each silk fiber segment was placed on a plastic "C" card, to prevent the small fiber from breaking during handling in diameter measurements and tensile testing. The "C" cards have a 19.5 mm rectangular cut-out on the side, the gauge length used in the analysis of mechanical properties. Each fiber was placed on the card along the cut out, taped, and glued at the inside edges of the card. Once the glue was dry an average diameter was obtained, from nine measurements at three different places in each fiber, under 40X magnification. A total of 190 silkworm silk fibers were carded and prepared

for testing. The fibers were organized by size of the spider silk gene insert, and number of generation (if more than one) F1 MiSp1-48, F1 MiSp1-64, F2 MiSp1-64, F1 MiSp1-HL, F2 MiSp1-HL, a non-transgenic group, and a native MiSp group.

After measuring all the diameters, tensile testing was conducted. The mechanical testing system (MTS) Synergie 100 was used for all tensile testing, with a 50 N load cell. Carded fibers were placed into the MTS aligning the fiber with the ends of the clips, and the side of the card was cut to allow the fiber, and the fiber alone, to be stretched. Some fibers broke during handling before they were tested and were removed from the analysis.

After the mechanical testing was completed a statistical analysis was conducted using SAS software to find if there were any statistically significant differences between the silk groups for each of the mechanical properties obtained through tensile testing. These tensile properties are: ultimate tensile strength, ultimate strain, energy to break, elastic modulus, and fiber diameter. A Ryan, Einot, Gabriel, Welch q (REGWQ) test was used to test for statistically significant differences in each of the silk groups. It is a stepwise comparison test, meaning the mean values of each groups are arranged in order from highest to lowest, and are compared based on how many steps they are apart from each other. The further apart the means are arranged, the larger the critical range has to be for there to be a statistically significant difference. The code written for this analysis can be seen in below:

```
data silk;
  input Group $ Energy_To_Break Ultimate_Tensile_Strength Ultimate_Strain
Diameter Elastic_Modulus;
  format Treatment $Char12.;
  label Energy_To_Break = "Energy to Break (MJ/m^3)";
  label Ultimate_Tensile_Strength = "Ultimate Tensile Strength (MPa)";
```

```
  label Ultimate_Strain = "Ultimate Strain (mm/mm)";
  label Diameter = "Diameter (um)";
  label Elastic_Modulus = "Elastic Modulus (GPa)";
  datalines;
* data is pasted or imported here *
;
run;

proc glm data = silk;
class Group;
model Energy_To_Break Ultimate_Tensile_Strength Ultimate_Strain Diameter
Elastic_Modulus = Group;
means Group / REGWQ;
run;
```

Genomic Analysis

For genomic extractions 30-40 mg of silk moth tissue were collected from each moth and genomic material was extracted using an E.Z.N.A.® Insect DNA Kit from Omega Bio-tek using 75 µl elutions. The purified genomic material was used to verify the presence of the spider silk gene in the silkworm genome through PCR. PCR primers were designed to target the outside part of the junctions in the genome where the spider silk genes were inserted. This is especially important for the hybrid fibers to tell the difference between the MiSp1 in the light chain and the MiSp1 in the heavy chain. Two types of PCR were conducted, long range PCR was used to confirm transgenicity by making long PCR products of about 12 kb for the MiSp1-48 and 14 kb for the MiSp1-64 inserts, and regular PCR was used to make PCR products of the sections in the silkworm genome surrounding the insert regions with sizes of ~900 bp for the light chain insert region and ~1.7 kb for the heavy chain insert region. PCR primer sequences used are in

Table 3. Longer primers were required for the long range PCR to help reduce some of the non-specific banding, but both the regular and long range version of the PCR primers cover the same DNA sequences. Primers for the LC were designed from the *Bombyx mori* Light Chain gene sequence with GenBank accession M76430.1, and Primers for the HC were designed in a previous project using the the *Bombyx mori* Heavy Chain gene sequence with GenBank accession AF226688.1.[48]

Table 3. PCR primer sequences used for PCR of the DNA insert and insert regions.

DNA Sequence	Primers	
Long Range LC insert	**Forward**	5'- GAGTCCATCGCGGACAAAACAACGTGACACGTG -3'
	Reverse	5'- CTAAGCCGGTCGCGTCATTACCGTTGCCAACGC -3'
Regular LC	**Forward**	5'- ATCGCGGACAAAACAACGTG -3'
	Reverse	5'- CTAAGCCGGTCGCGTCATTA -3'
Long Range HC insert	**Forward**	5'- TTCAGAAGGTGGCCAGACGATATCACGGGCCAC -3'
	Reverse	5'- CGCTTCCTACTCCTTGTCCGTACCCAGCGCCAG -3'
Regular HC	**Forward**	5'- GGCCAGACGATATCACGGGC -3'
	Reverse	5'- TTGTCCGTACCCAGCGCCAG -3'

Regular PCR was conducted for each gene from template plasmids using a Phusion® High-Fidelity PCR Master Mix with HF Buffer from NEB. Solutions were set up in 0.2 ml flat cap tubes. Each solution had 5.5 µl of ddH2O, 2.5 µl (5 µM) of the corresponding reverse primer, 2.5 µl (5 µM) of the corresponding forward primer, 2 µl of the corresponding genomic DNA template, and 12.5 µl of the Phusion® High-Fidelity

PCR Master Mix. The reactions were set up for 35 cycles with a 10 second denaturation time at 98 °C, a 30 second annealing time at 57 °C, and a 30 second (for LC insert region) or 45 second (for HC insert region) extension time at 72 °C, as well as an overall initial 30 second denaturation time at 98 °C and a final 5 minute extension time at 72 °C.

Long range PCR was conducted using a TaKaRa LA Taq® PCR kit from TAKARA BIO INC. Solutions were set up in 0.2 ml flat cap tubes. Each reaction had had 5 µl of ddH2O, 2.5 µl (10 µM) of the corresponding reverse primer, 2.5 µl (10 µM) of the corresponding forward primer, 3 µl of the DNA template, 4 µl of dNTPs, 2.5 µl of $MgCl_2$, 5 µl 10X buffer, and 0.5 µl of TaKaRa LA Taq® polymerase. The reactions were set up for 35 cycles with a 10 second denaturation time at 98 °C, and a 15 min annealing/extension time at 68 °C, as well as an overall initial 1 minute denaturation time at 94 °C and a final 10 minute extension time at 72 °C.

The combination of long range PCR and regular PCR was used to verify the biallelic status of the transgenic silkworm genomes. Agarose gel electrophoresis was performed on the PCR solutions to visualize and analyze the PCR product bands, using 1% agarose gel run at 100 V for 35 minutes. Bands from the long range PCR corresponded to transgenic genomes while bands from the regular PCR corresponded to non-transgenic genomes. Since there are two alleles present in each genome, the long range PCR bands with regular PCR bands present in the gels corresponded to heterozygous transgenic genomes, and long range PCR bands with no regular PCR bands present corresponded to homozygous transgenic genomes.

Protein Analysis

Attempts for protein analysis through SDS page and Western blot were as follows. Several methods were used to attempt to dissolve the silk fibers. A 9 M solution of LiSCN was used to successfully dissolve the silk. 10 mg of each group of silk were placed in microcentrifuge tubes with 500 µl of 9 M LiSCN and placed in a water bath at 70 °C for 2 hours. The silk solutions were centrifuged at 14000 rpm for 2 minutes and the supernatant was used for SDS PAGE. 300 µl of each silk solution were placed into 15 kDa MWCO dialysis tubing and dialyzed against 1 L of 50 mM ammonium bicarbonate at 4 °C overnight. The dialyzed solution was pipetted into microcentrifuge tubes and centrifuged at 14000 rpm for 2 minutes. The supernatants were placed into clean microcentrifuge tubes, and the remaining pellet was allowed to dry. The pellet was then re-dissolved with 8 M urea and 2% sarkosyl by sonication with a microtip for 10 seconds at 1 amp.

SDS-PAGE was done to separate proteins by size and transfer them to a membrane for Western blotting to confirm the correct size bands are the spider silk proteins. Samples of the dissolved silk were prepared by taking 50 µl of silk solution in microcentrifuge tubes and adding 50 µl of 2x Laemmli Sample Buffer from Bio-Rad Laboratories with β-mercaptoethanol. A solution of GFP from Millipore Sigma was Sample used as a control and was prepared by mixing 10 µl (1 µg/µl) with 10 µl of 2x Laemmli Buffer. The solutions were boiled for 15 minutes and then centrifuged for 2 minutes. The solutions were loaded into the wells of a Novex™ 4-20% Tris-Glycine Mini Gel from Thermo Fisher Scientific in volumes of 5-25 µl and run at 100 V for 90

minutes with a tris glycine running buffer. The running buffer was made by dissolving 3 g of Tris, 14.4 g of glycine, and 1 g of SDS in 1 L of ddH_2O.

The gel was then transferred onto a polyvinylidene difluoride (PVDF) membrane which was first activated by soaking in methanol for 1 minute. The "sandwich" for transfer was put together starting from the black side (negative side) of the cassette with 2 sponges, 2 filter papers, the gel, the PVDF membrane, 2 more filter papers, and 2 more sponges. The cassette was closed together and placed into the transfer box with transfer buffer. The transfer was done at 4 °C overnight at 40 V and then at 100 V 1 hour. The transfer buffer was made using 3 g of Tris, 14.4 g of glycine, and 100 ml of methanol in 1 L of ddH_2O. One additional attempt was conducted using a transfer buffer with 200 ml of methanol instead of 100 ml.

After the transfer was completed, the gel was stained with Coomassie to assess how well the proteins transferred from the gel onto the membrane using a standard Coomassie stain for 1 hour and then de-stained for 1 hour. The PVDF membrane was blocked in TBST with 5% milk for 1 hour at room temperature, then rinsed in 3 washes of TBST for 10 minutes each. The membrane was then incubated at room temperature for 1 hour with the primary antibody diluted 1:1000 in TBST with 5% milk. An eGFP monoclonal antibody from Thermo Fisher Scientific was used as the primary antibody for all the groups. The membrane was rinsed again in 3 washes of TBST for 10 minutes each, and then incubated in with the secondary antibody diluted 1:1000 in TBST with 5% milk. The membrane was rinsed once again in 3 washes of TBST for 10 minutes each. The membrane was then developed with a 1-Step™ NBT/BCIP Substrate Solution from Thermo Fisher Scientific.

Hexafluoroisopropanol (HFIP) was also used to dissolve the silk fibers. 10 µg of degummed silk were placed in 4 ml solutions of HFIP and HFIP + 10% β-mercaptoethanol were used to attempt to dissolve the silk. A solution of calcium chloride, ethanol, and water at a molar ratio of 1:2:8 was also used to attempt to dissolve the silk. These solutions were rotated for over 30 days and sonicated at 1 amp, for 30 seconds at a time, about once a week to attempt to solubilize the silk proteins, but none completely solubilized the silk fibers. Gland material was also collected by dissecting the silk glands from a silkworm at the 5th instar and dissolving sections of the gland in 8M urea and 8M urea and 2% sarkosyl. SDS-PAGE was attempted, however, the silk solutions gelled completely after adding the loading buffer and boiling for 5 minutes.

Dot blots were attempted from the HFIP silk solutions, LiSCN solution, and the 8M urea + 2% sarkosyl solution (from the dialyzed pellet). A nitrocellulose membrane was used for the dot blot by drawing a grid of 1x1 cm squares and creating a series of dilutions for the dissolved silk. GFP was used as a positive control and bovine serum albumin (BSA) was used as a negative control. The initial concentrations for the controls were 0.2 µg/µl for GFP, 1 µg/µl for BSA. 10 µl of each solution were diluted in 90 µl of the corresponding solvent for the first 1:10 dilution, the 1:100 dilution was made by diluting 10 µl of each 1:10 dilution into 90 µl, and the final 1:1000 dilution was made using 10 µl of the 1:100 solution in 90 µl. 5 µl of each dilution were used to make a single dot within the grid on the membrane, and the membrane was allowed to dry before following the same Western blot process described above.

A densitometry analysis was then conducted on the dot blot from the 8M urea + 2% sarkosyl solution. An image was taken of the membrane and analyzed with imageJ

to obtain an area intensity value (of arbitrary units) for each dot. The control GFP dots were used to create a standard curve to calculate the amount of GFP present in the silk sample. The standard curve was calculated by normalizing the area intensity values to percent values based on the known concentrations of the GFP control dots with the 0.2 µg/µl concentration of GFP standardized to 100% and the 0.02 µg/µl and 0.002 µg/µl concentrations according to the area intensity of each dot. The percent concentrations were plotted against the known w/v concentrations of each control dot, and a best fit curve was found using excel.

The concentrations of eGFP in the silk samples were calculated from the standard curve equation, based in the percent area intensity of each sample. The eGFP concentrations were then correlated to a MiSp1 concentration based on the size ratio of the eGFP protein to the attached MiSp1 48 or MiSp1 64 proteins. For MiSp1 48 the ratio is 195 kDa/27kDa = 7.2, and for MiSp1 64 the ratio is 252 kDa/27kDa = 9.3. Each eGFP concentration was multiplied by its corresponding ratio to calculate approximate concentrations of dissolved MiSp1 protein in the transgenic silk samples.

Polarized Light Microscopy

Fibers were carded in the same way as for the mechanical testing, except using large bundles of fibers instead of a single fiber. One card was made for each of the silk groups, and each card had a ~0.5 cm wide mat of aligned fibers glued onto it.

A petrographic microscope was used to observe the fiber mats under polarized

light, and to rotate the fibers from 0 ° to 45° to see the change in the refringence of light through the fibers at the different degrees of orientation. Images were taken at 0 ° and 45° and then compared. The fibers with the highest observed change in refringence (birefringence), were inferred to have more orientation within the crystalline structures. Since crystalline structures in the silk are largely responsible for the mechanical properties of the silk, a qualitative analysis was done comparing the observed change in refringence of the silk samples to the mechanical properties of each silk group.

RESULTS AND DISCUSSION

Preliminary Analysis

Through an analysis of the repetitive motifs in the MiSp1 and MaSp1 amino acid sequences, it was found that MiSp1 without the spacer region is approximately 60% crystalline, and MaSp1 is approximately 24% crystalline. A linear relationship was created of the predicted percent crystallinity in the silk fibroin with increasing spider silk content. Non-transgenic silk fibroin was assumed to be 50% crystalline based on a previous study.[50] Figure 6 and Table 4 compare the potential percent crystallinity increase with increased spider silk content between MiSp1 and MaSp1. Due to the highly crystalline nature of MiSp1, the percent crystallinity of the transgenic silk fibroin increases much more quickly than with MaSp1. While the silk fibroin would only need a 30% addition of MiSp1 to reach 68% crystallinity, it would need a 75% addition of MaSp1 to reach the same percent crystallinity. Although there are many more factors that influence the mechanical properties of silk, such as the size and composition of the beta sheet structures in the silk and the efficacy of the silkworms producing the silk, the quick increase in crystallinity with the addition of MiSp1 is a good indication of how drastically the mechanical properties of the silk fibroin could be changed, even with small increases of the spider silk content in the fiber.

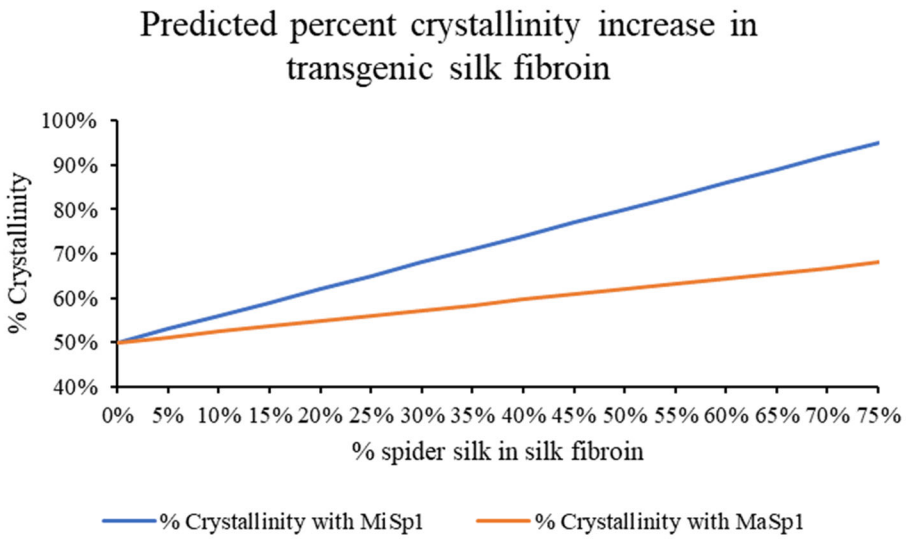

Figure 6. Comparison of predicted increase in percent crystallinity of silk fibroin with addition of MiSp1(blue) or MaSp1 (orange) in the light chain.

Table 4. Predicted percent crystallinity increase with increasing spider silk content.

Percent spider silk in silk fibroin	% Crystallinity with MiSp1	% Crystallinity with MaSp1
0%	50%	50%
5%	53%	51%
10%	56%	52%
15%	59%	54%
20%	62%	55%
25%	65%	56%
30%	68%	57%
35%	71%	58%
40%	74%	60%
45%	77%	61%
50%	80%	62%
55%	83%	63%
60%	86%	64%
65%	89%	66%
70%	92%	67%
75%	95%	68%

DNA Plasmid Construction

Ligations of 16 and 32 repeats of the MiSp1 gene were performed to make units of 48 and 64 repeats of the MiSp1 gene. Sequential digestions were performed with AgeI and BspEI on plasmids containing the 16 and 32 repeats of the MiSp1 gene, run through an electrophoresis gel to separate the MiSp1 gene from the vector and purified from the gel. A single digestion was conducted with BspEI on only the plasmid with 32 repeats of the MiSp1 gene, to linearize the vector for ligation. The MiSp1 48 repeat was made by ligating the MiSp1 16 gene with the MiSp1 32 linearized plasmid, and the MiSp1 64 repeat was made by ligating the MiSp1 32 gene with the MiSp1 32 linearized plasmid, as seen in Figure 7 below.

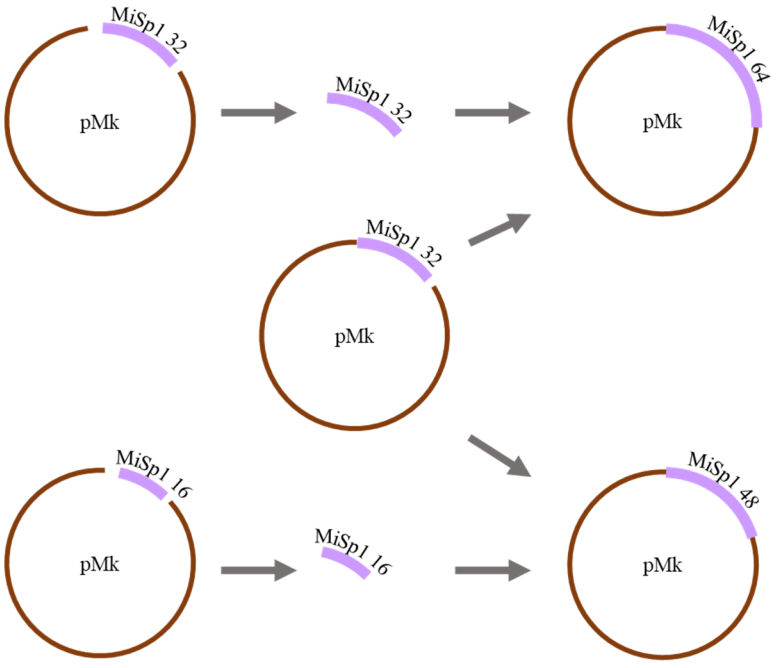

Figure 7. Graphic of MiSp1 64 and MiSp1 48 ligations from MiSp1 32 and MiSp1 16 in a pMk plasmid.

The ligations were transformed into TOP10 competent cells, 12 colonies from each transformation were selected and successful ligations were verified through gel electrophoresis after double digestions. Figure 8 shows the gel images of the MiSp1 48 and MiSp 64 ligation plasmid checks. The top image shows the correct size of bands for the MiSp1 64 plasmid in lanes 1 and 2 (~9.4 kb), while the bottom image shows the correct size band (~7.1 kb) for the MiSp1 48 plasmid in lane 4.

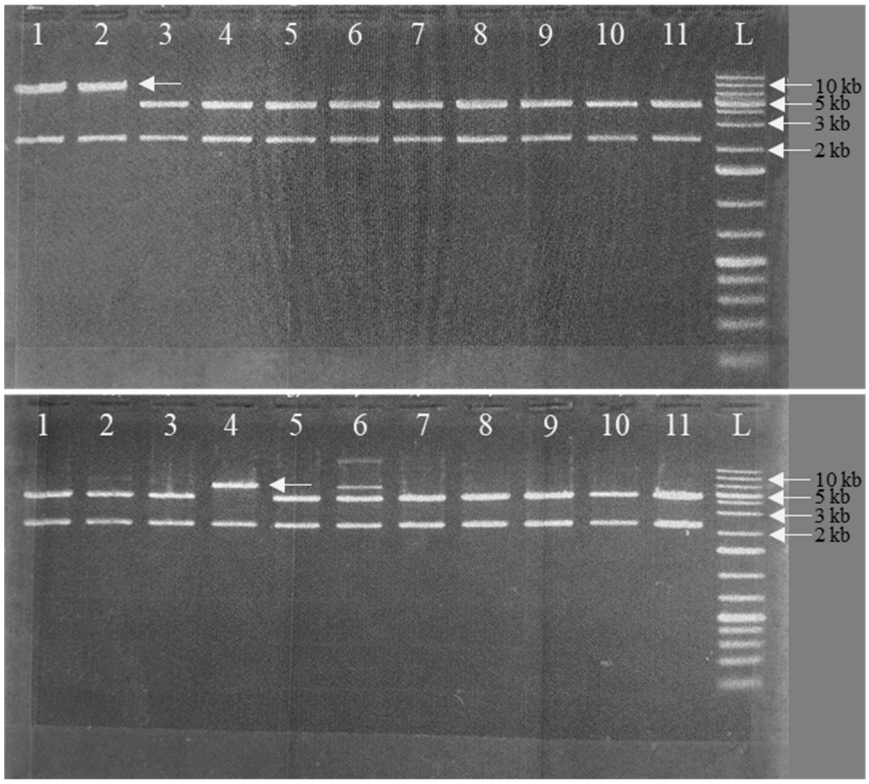

Figure 8. Gel electrophoresis images of plasmid digestions checks for the correct ligations of MiSp1 64 and MiSp1 48. Lanes 1 and 2, panel A, show the correct size band for MiSp1 64 ligation, around 9.4 kb, Lane 4 in B shows the correct size band for MiSp 48 ligation, around 7.1 kb.

Since the restriction enzymes used to construct the MiSp1 48/64 plasmids have compatible cohesive ends, the plasmids were sent for sequencing to make sure the MiSp1 genes were ligated together in the correct orientation. Sequencing results were compared to the MiSp1 sequence to make sure the ligation was correct. After verifying the MiSp1 gene ligations were correct, the NTD and CTD genes were ligated into the pBlue vector which already contained the eGFP gene insert. After the NTD sequence was amplified through PCR it was digested with KpnI and SalI to create the sticky ends and inserted into the vector which was also digested with the same enzymes, resulting in a 4.4 kb plasmid.

This plasmid was transformed into TOP10 competent cells for amplification. Then the amplified plasmid was prepared for ligation with the CTD. Like the NTD, the CTD sequence was amplified through PCR, but was digested with BamHI and SacI restriction enzymes. The vector now containing the NTD sequence was also digested with the same enzymes and ligated with the CTD. Figure 9 shows the ligations of the NTD and CTD genes in to the expression plasmid as well as DNA gel images containing digestions of the correct ligations.

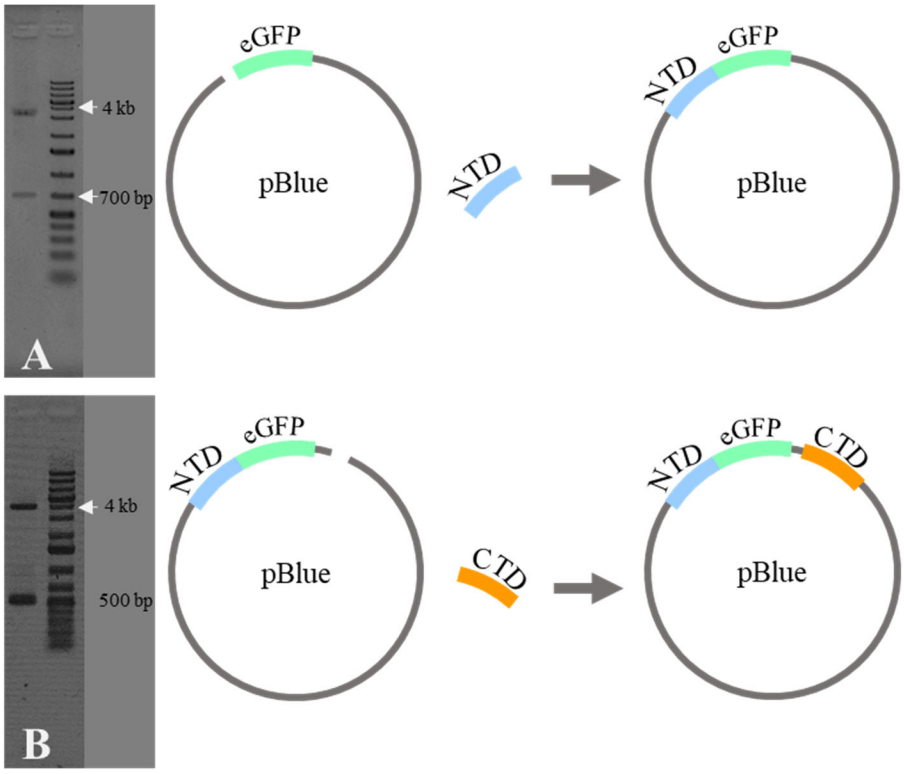

Figure 9. A) Gel showing the correct ligation for the NTD in the pBlue vector containing the eGFP gene, next to the drawing showing the ligation into the expression vector. B) Gel showing the correct ligation for the CTD in the pBlue vector containing the eGFP gene and the NTD gene from the previous ligation, next to the drawing showing the ligation.

The completed vector (PBlue+NTD+eGFP+CTD), and the MiSp1 48/64 plasmids were then digested with HindIII and BamHI to prepare it for the ligations. An electrophoresis gel was run for the MiSp1 digestions to separate them from the pMK vector, before purifying the DNA segments and performing the ligations. After transforming the cells, and collecting the DNA, gel electrophoresis was done to identify the correct ligations. Figure 10 shows the gels for the MiSp1 48 gene and MiSp1 64 gene in the expression plasmid. At the time the digestion was done for the MiSp 48 ligation check there was no HindIII restriction enzyme available, so the digestion was

done with BamHI and SalI which resulted in bands containing the eGFP+MiSp1 48 (~7.7 kb) and pBlue+NTD+CTD (~4.2 kb). HindIII was available at the time for the MiSp1 64 ligation check, so the digestion was done with BamHI and HindIII and the resulting bands were of MiSp1 64 (~9.4 kb) and the vector pBlue+NTD+eGFP+CTD (~4.9 kb).

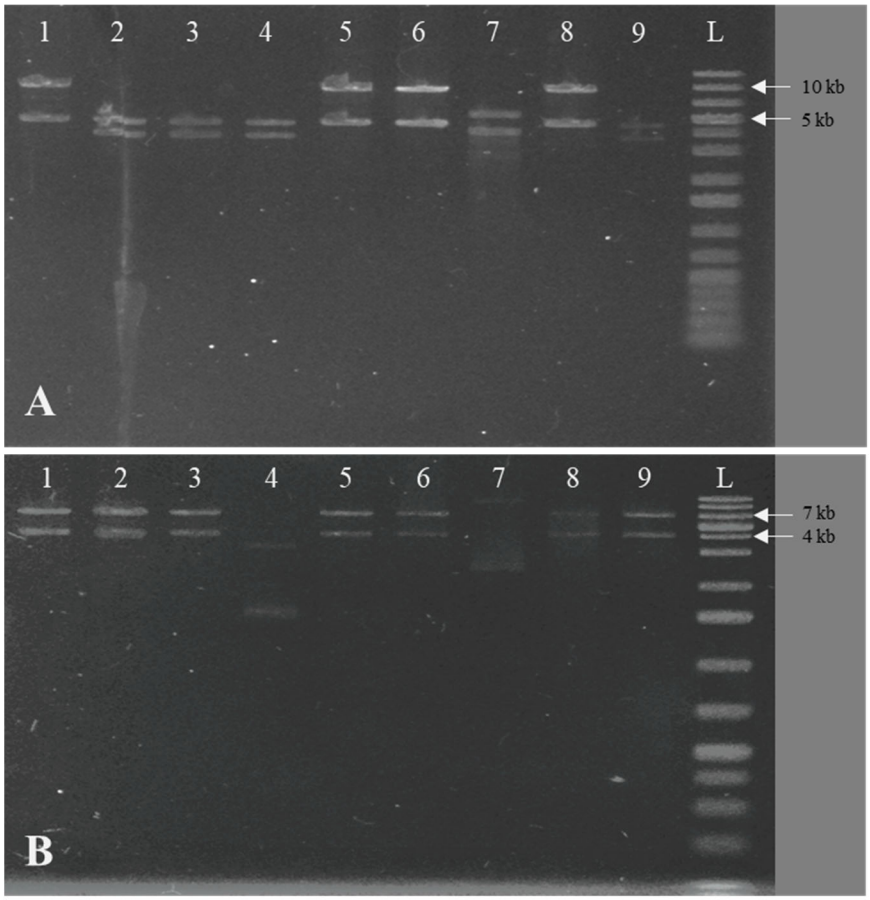

Figure 10. A) MiSp1 64 digestion check done with HindIII and BamHI restriction enzymes. Correct ligation in lanes 1, 5, 6, 8 show top band with MiSp1 64 segment (~9.4 kb) and bottom band containing expression vector pBlue+NTD+eGFP+CTD (~4.9 kb). B) MiSp1 48 digestion check done with SalI and BamHI restriction enzymes. Correct ligations in lanes 1, 2, 3, 5, 6, 8, 9 show top band containing eGFP+MiSp1 48 (~7.7 kb) and bottom band containing the remaining expression vector pBlue+NTD+CTD (~4.2 kb).

Electroporation and Sericulture

Electroporation of freshly laid non-transgenic silkworm eggs was conducted following construction of the expression plasmid and the amplification of the Cas9 and gRNA plasmids. The electroporated eggs were placed in appropriate conditions to develop and hatch. It took 10-12 days for the eggs to hatch after the electroporation and a hydrochloric acid treatment to disrupt the eggs' diapause period. The newly hatched silkworms were raised until they made cocoons, which took about 30 days. Then the cocoons were examined under UV light to determine which cocoons glowed green, indicating the silkworms that were successfully genetically modified. The pupae were removed from the brightest glowing cocoons and allowed to hatch and breed for the next generation. At the same time, the cocoons were degummed and prepared for mechanical testing. Figure 11 shows the progression from electroporation of the eggs through the moth stage.

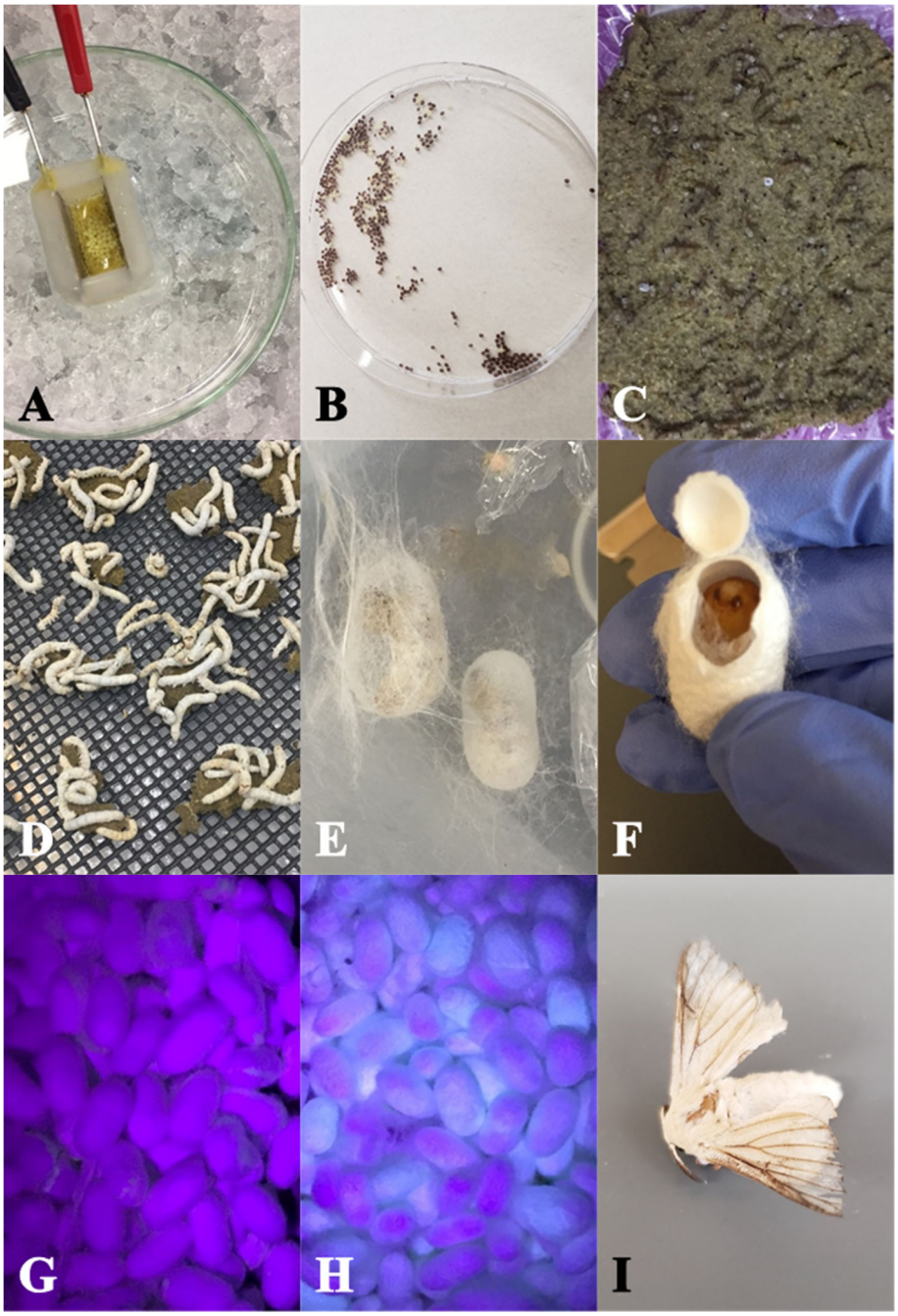

Figure 11. A) Picture of silkworm eggs submerged in the electroporation solution, in the electroporation cuvette. B) Developing silkworm eggs changed from yellow to dark grey. C) Newly hatched silkworms about 1 day old. D) Silkworms at 4th instar. E) silkworms beginning to make cocoons. F) Cut cocoon to observe pupae. G) Non-transgenic cocoons under UV light. H) Transgenic cocoons glowing green under UV light due to eGFP reporter protein. I) Adult transgenic silk moth, ready to mate and lay eggs for the next generation of transgenic silkworms.

Some of the F1 MiSp1 64 moths were mated with a different transgenic group of silkworms which had the MiSp1 (also with 64 repeats) gene in the heavy chain (HC) region of the silkworm genome, resulting in a hybrid group with the MiSp 1 in both the HC and LC regions of the silkworm region, potentially doubling the amount of spider silk in the silkworm silk. The hybrid transgenic groups were labeled MiSp1 HL. Finally, a total of 5 different transgenic groups were collected, 3 regular transgenic groups with the MiSp1 in only the LC, and 2 with the MiSp1 in the HC and LC. The groups were labeled as follows, with F1 and F2 marking the corresponding generation: F1 MiSp1 48, F1 MiSp1 64, F2 MiSp1 64, F1 MiSp1 HL, and F2 MiSp 1 HL

Mechanical Data Analysis

The carded fibers were set up in the MTS seen in Figure 12. The fibers were aligned parallel with the clamps, the top clamp was tightened, and the card edge was cut to allow the fiber to be tested, Due to human error, not every fiber was loaded onto the MTS tested correctly and these fibers were not included in the analysis. Errors included, slipping from not tightening the clamp enough, not cutting the card before testing, and breaking the fiber before testing. In each case the fiber was stretched or broken before accurate data could be collected.

Figure 12. Carded fiber set up in MTS.

Mechanical data were collected, and analyzed using Excel, for ultimate tensile strength, ultimate strain, energy to break, and elastic modulus. The analyzed data was compared to native silkworm silk group and a native spider silk MiSp group through statistical analysis. It is important to note that naturally spun silk is highly variable due to the way the silkworms spin it, and the properties of silk from the same cocoon can vary quite dramatically.[51] This variability in the silk's properties explains the low R-square values calculated in the statistical analysis and the presence of so many outliers in the distribution of the data for each group. The removal of the fibers from the groups, from inaccurate testing, resulted in a total of 169 analyzed fibers with 23-30 fibers in each group, except for the native MiSp group for which only 10 fibers were tested and 9 used in the analysis. The average mechanical properties for the silkworm groups are summarized in Table 5 below.

Table 5. summary of silk mechanical properties.

	Energy to Break (MJ/m^3)	Max Stress (MPa)	Max Strain (mm/mm)	Diameter (µm)	Elastic Modulus (GPa)
F1 MiSp1 48	211.36 ± 57.98	905.09 ± 162.99	0.34 ± 0.06	7.0 ± 0.4	9.05 ± 1.82
F1 MiSp1 64	207.75 ± 77.62	912.54 ± 130.25	0.33 ± 0.08	7.4 ± 0.7	9.00 ± 1.11
F1 MiSp1 HL	196.74 ± 74.63	842.20 ± 153.17	0.33 ± 0.09	8.7 ± 0.5	8.91 ± 0.82
F2 MiSp1 64	141.94 ± 67.31	646.67 ± 125.76	0.31 ± 0.09	8.7 ± 0.7	6.89 ± 1.26
F2 MiSp1 HL	237.89 ± 81.09	1107.92 ± 165.5	0.28 ± 0.08	7.0 ± 0.4	11.15 ± 2.20
Native Silkworm silk	173.80 ± 47.44	784.90 ± 114.35	0.32 ± 0.06	8.5 ± 0.8	7.75 ± 1.30
Native MiSp	90.63 ± 21.48	1196.88 ± 112.31	0.13 ± 0.02	4.7 ± 0.1	12.07 ± 1.93

Starting with ultimate tensile strength, or maximum stress, the transgenic silk group with the highest mean was the F2 MiSp1 HL group, at 1107.92 MPa, and was statistically higher than every other group, except for the native MiSp which had a mean of 1196.88 MPa. The F2 MiSp1 64 group had the lowest ultimate tensile strength of all the groups at 646.67 MPa, including the native Silkworm group with a mean of 784.90 MPa, and it was statistically lower than all other groups. F1 MiSp1 48 (905.09 MPa) and F1 MiSp1 64 (912.54 MPa) both showed an increase of around 120 MPa compared to the native Silkworm group, and the F1 MiSp HL (842.20 MPa) had a less than 60 MPa increase. The F1 MiSp HL group was the only group in the ultimate tensile stress analysis that was not statistically different than the native silkworm group. A bar chart with statistical significance in ultimate tensile strength shown in Figure 13 below.

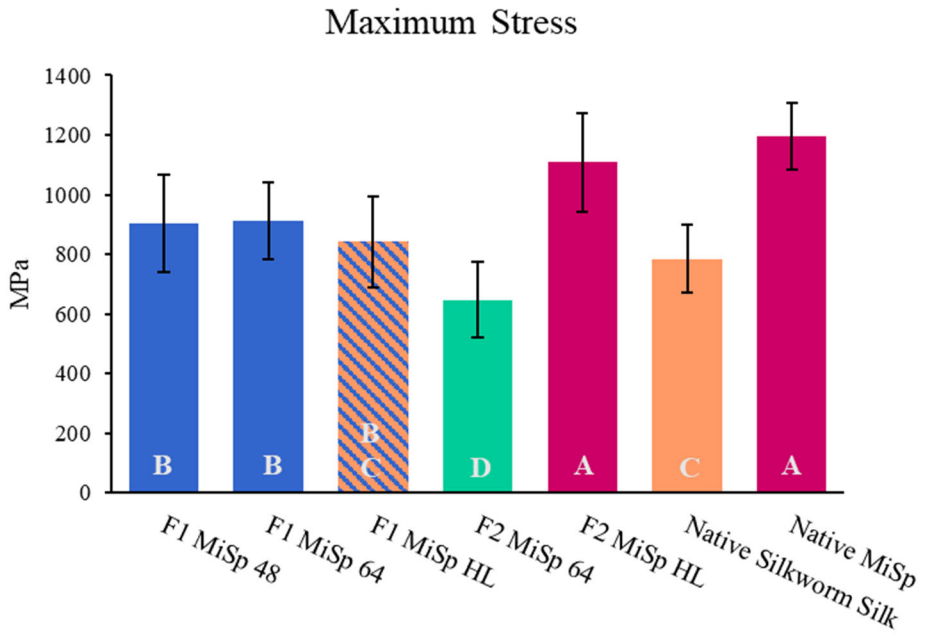

Figure 13. Average ultimate tensile strength values with standard deviations by group. Groups with the same letter/color are not statistically significantly different.

The low strength of the F2 MiSp1 64 group of transgenic worms is likely due to unhealthy growth conditions caused by a mold outbreak introduced into the silkworm room through contaminated silkworm food. It is likely the worms were unable to spin cocoons as effectively which resulted in weak silk, regardless of the presence of the spider silk protein. If the worms were unable to pull the silk enough when spinning, then it is possible the proteins were not aligned properly to achieve optimal mechanical properties.

While diameters alone are not a central mechanical property, they can highlight the significance of other mechanical properties, since diameter is taken into the calculations for maximum stress. The effectiveness of silk spinning could be influencing fiber diameter, which is important in the ultimate tensile strength calculations. In this

analysis there were 3 separate groups of statistical significance. Native MiSp had the lowest mean diameter at 4.7 µm and was statistically different than the rest of the groups. F2 MiSp HL, F1 MiSp 64, and F1 MiSp 48 were all in the same statistical group with mean diameters between 7.0 µm and 7.4 µm. Finally, the native Silkworm, the F1 MiSp HL and the F2 MiSp 64 groups were in the same statistical group with mean diameters between 8.5 µm and 8.7 µm. A bar chart with statistical significance can be observed in Figure 14 below for average diameters.

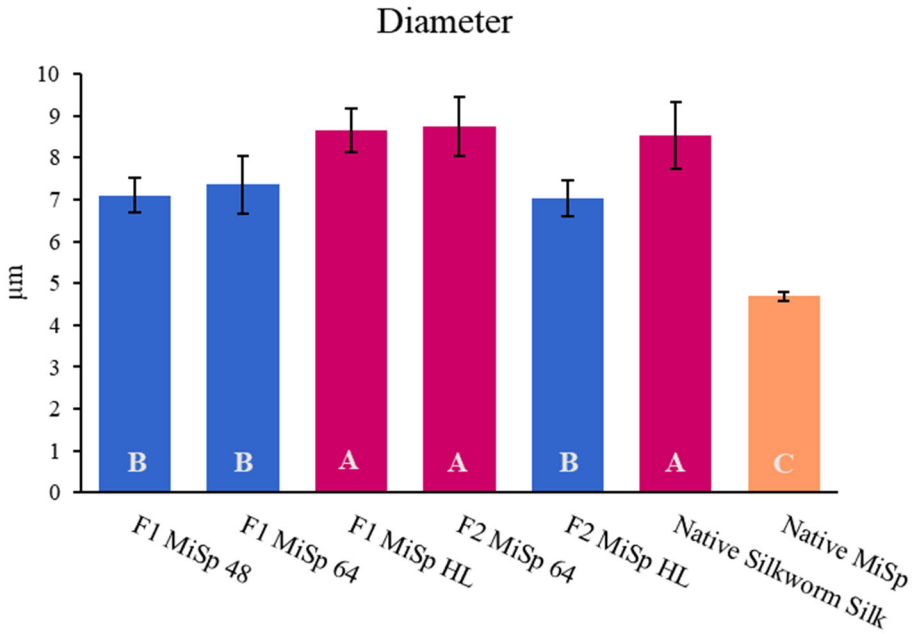

Figure 14. Average diameter values with standard deviations by group. Groups with the same letter/color are not statistically different.

While the statistical analysis was conducted within each mechanical property, and not between the properties, there was an observed relationship between diameter

and ultimate tensile strength. The silk groups with smaller diameters tend to have a higher tensile strength. The native MiSp had the lowest mean diameter but the highest mean ultimate tensile strength out of all the groups, while the F2 MiSp 64 group had the highest mean diameter but the lowest mean ultimate tensile strength. Although there is an observed correlation between diameter and ultimate tensile strength, there are many more factors that influence the mechanical properties of silk, from the amino acid composition and secondary structure, to the health of the worms and their effectiveness at spinning.

The only statistical difference in ultimate strain was between the native MiSp and the rest of the tested groups, with the mean maximum strain for the native MiSp being 0.13 mm/mm and the mean maximum strain for the rest of the groups ranged from 0.28mm/mm to 0.34 mm/mm, over double the maximum stress of the native MiSp silk. Ultimate strain averages with statistical analysis can be seen in Figure 15.

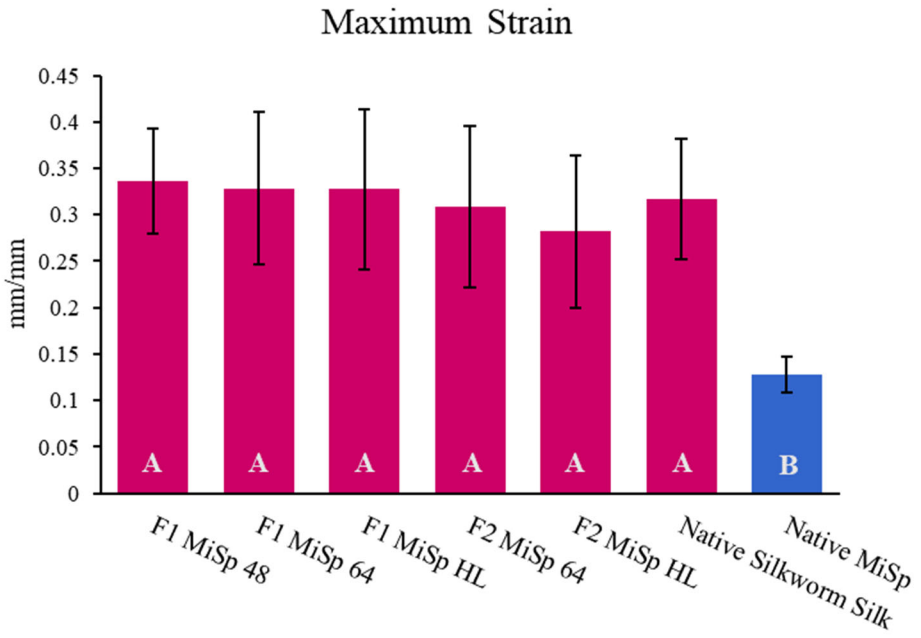

Figure 15. Average ultimate strain values with standard deviations by group. Groups with the same letter/color are not statistically significantly different.

The integration of a stress vs. strain curve yields the energy required to break a fiber. Changes in either the ultimate tensile strength or ultimate strain will have a great impact on the energy to break, as observed in these data. The combination of high ultimate tensile strength and low ultimate strain in the native MiSp fibers resulted in the lowest energy to break at 90.63 MJ/m^3, statistically different from the rest of the groups. F2 MiSp1 64, native silkworm, and F1 MiSp1 HL were in the next group of statistical significance; these groups of fibers had the lowest values of ultimate tensile strength. In the next group of statistical significance were native silkworm, and all the transgenic F1 groups, with energy to break values of between 173.80 MJ/m^3 for the native silkworm fibers and 211.36 MJ/m^3 for the F1 MiSp48 group. In the final group of statistical significance for energy to break with the highest mean values, were all the F1 groups

and the F2 MiSp1 HL group, ranging from 196.74 MJ/m^3 for the F1 MiSp1 HL to 237.89 MJ/m^3 for the F2 MiSp1 HL. The F2 MiSp1 HL and the native MiSp groups were the only test groups to be statistically significantly different from the native Silkworm group, with F2 MiSp1 HL having the highest energy to break, and native MiSp with the lowest energy to break. Figure 16 shows the average values, and statistical significance of the energy to break groups.

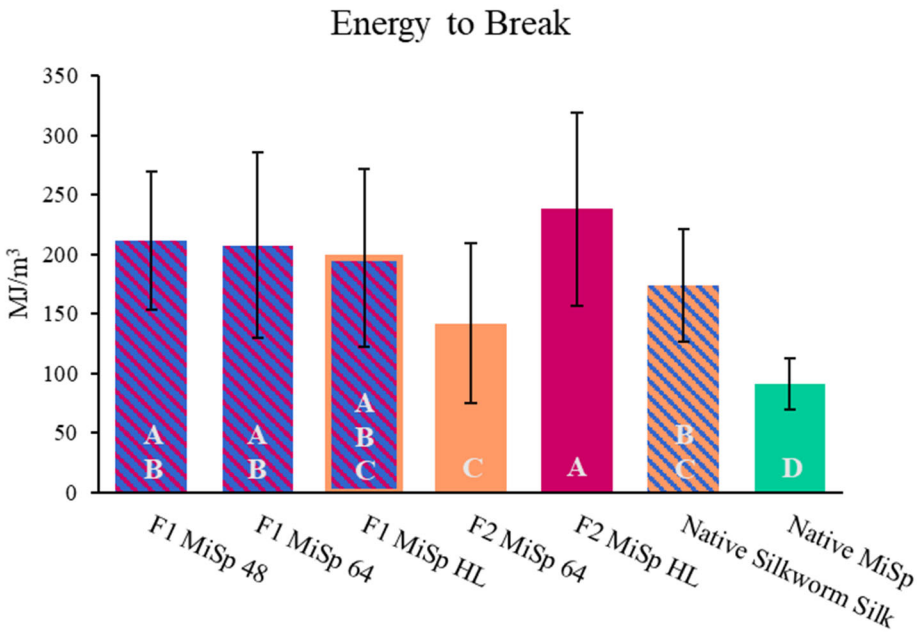

Figure 16. Average energy to break values by group. Groups with the same letter/color are not statistically significantly different.

Although F1 MiSp1 HL was in 3 statistical groups, there was a much larger difference between this transgenic group and the Silkworm and F2 MiSp1 64 group, than between the other F1 groups. This broad range of statistical significance between

the statistical groups is likely due to the high variability in silk mechanical properties within each group and is even more pronounced in this case since the energy to break is calculated from ultimate stress and ultimate strain. Likewise, the combination of high stress and high strain resulted in the high energy to break observed in F2 MiSp1 HL (173.80 MJ/m^3), while the native MiSp (90.03 MJ/m^3) resulted in the lowest energy to break due to the silk's low strain despite having the highest tensile stress.

Despite there being no statistical differences in the maximum strain of the transgenic silk groups, the differences in ultimate tensile strength were large enough to create statistically differences in the energy to break. The combination of high strain from the silkworm silk and high strength from the MiSp1 inserts resulted in the high energy to break of the transgenic groups (with the exception of the F2 MiSp1 64 group of worms which were unhealthy and unable to spin strong silk) especially when compared to native MiSp (90.03 MJ/m^3) which had a low energy to break due to its low ultimate strain.

Elastic modulus is another factor that is influenced by both stress and strain; it is a measure of how much force can be applied to a material as it is being stretched before it is permanently deformed and is calculated as the slope of the elastic deformation region. The expectation when analyzing the mechanical data was to see an increase in elastic modulus (meaning the silk would be less elastic) with increasing MiSp1 content. Although there was no statistical difference between the F1 groups and the native Silkworm group, the F2 MiSp1 HL group showed a significant increase in elastic modulus and was covered in the same statistical group as the native Native MiSp. The Native MiSp group had a mean of 12.07 GPa while the F2 MiSp1 HL group had a

slightly lower mean elastic modulus at 11.15 GPa. The F2 MiSp 64 and the Native Silkworm groups had the smallest mean elastic modulus values and were placed in the same statistical group with mean elastic modulus values of 6.89 GPa and 7.75 GPa respectively. The heavy chain protein in the fibroin is similar in crystallinity to the MiSp1 protein, while the light chain protein is more like the MiSp1 spacer motif, so by incorporating the MiSp1 protein without the spacer it was expected to get fibers with a high elastic modulus. Figure 17 contains the average values and statistical significance for elastic modulus.

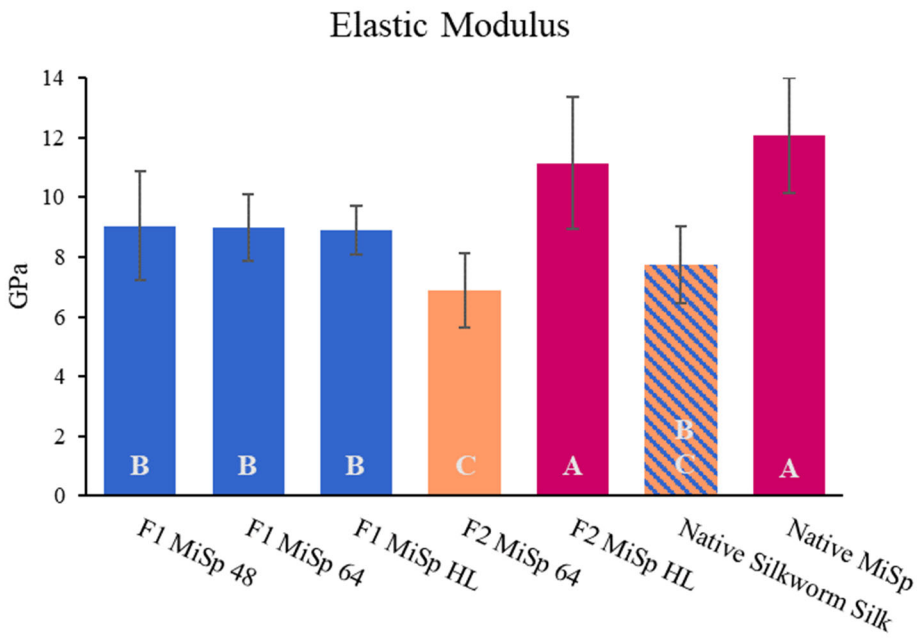

Figure 17. Distribution of elastic modulus values by group. Groups with the same letter are not statistically significantly different.

Mechanical properties were increased in all the transgenic groups except for the F2 MiSp1 64 group, which had lower mechanical properties than even the native silkworm silk. The decreased mechanical properties were most likely due to the mold outbreak which caused most of the silkworms in the F2 MiSp1 64 and all the F2 MiSp1 48 groups to die. It was assumed that the silkworms were infected through silkworm chow contaminated with mold spores, as even autoclaving the food and all other measures to prevent any contamination to the silkworm room did not prevent the infection.

Only a few silkworms from the F2 MiSp1 64 group survived long enough to make cocoons, but eventually died as pupae and were covered in mold. As mentioned before, it is possible that the silkworms were too weak to spin their silk properly and stretch the silk fibers enough to achieve the optimal protein alignment for high mechanical properties. The slightly larger diameter, low ultimate tensile strength, low energy to break, and low elastic modulus are all indicative of the silkworms' inability to spin and stretch the silk appropriately for the secondary structures in the proteins to align properly.

To assess the protein alignment in the silk fibers, silk bundles from each group were placed under a petrographic microscope. This microscope has two polarizing planes oriented perpendicular to each other. Crystalline structures such as those in the silk change the direction of the polarized light, allowing it through to the viewer, where an isotropic material would block the light completely. The silk fibers were aligned parallel with one of the polarizers, at 0° and then at 45° from each polarizer. At 0° crystalline structures are aligned with only one of the polarizers letting minimal light

through the fibers, and at 45° the crystal structures in the silk let the most amount of light through. The maximum change in refringence of the silk at different polarization orientations is called birefringence. In this case, higher birefringence means higher crystalline structure orientation which results in increased mechanical properties of the fiber, particularly in tensile strength.

Images of the silk fibers were taken at each orientation, 0° and 45 °. Figure 18 shows the change of refringence of the silk groups. The native MiSp and native silkworm silk groups were used as a positive and negative control respectively. The maximum change in refringence was observed in the native MiSp silk, with the F2 MiSp1 HL silk group showing a similar change. The F2 MiSp1 64 group, however, did not show a significant change in refringence between the two orientations which means that the crystalline structures in this group of silk were not as aligned as even the native silkworm silk, which resulted in the group's low mechanical properties. In contrast, the silk groups with the most marked change in refringence from 0° to 45° were the native MiSp and the F2 MiSp1 HL groups which had the highest tensile strength of all the groups.

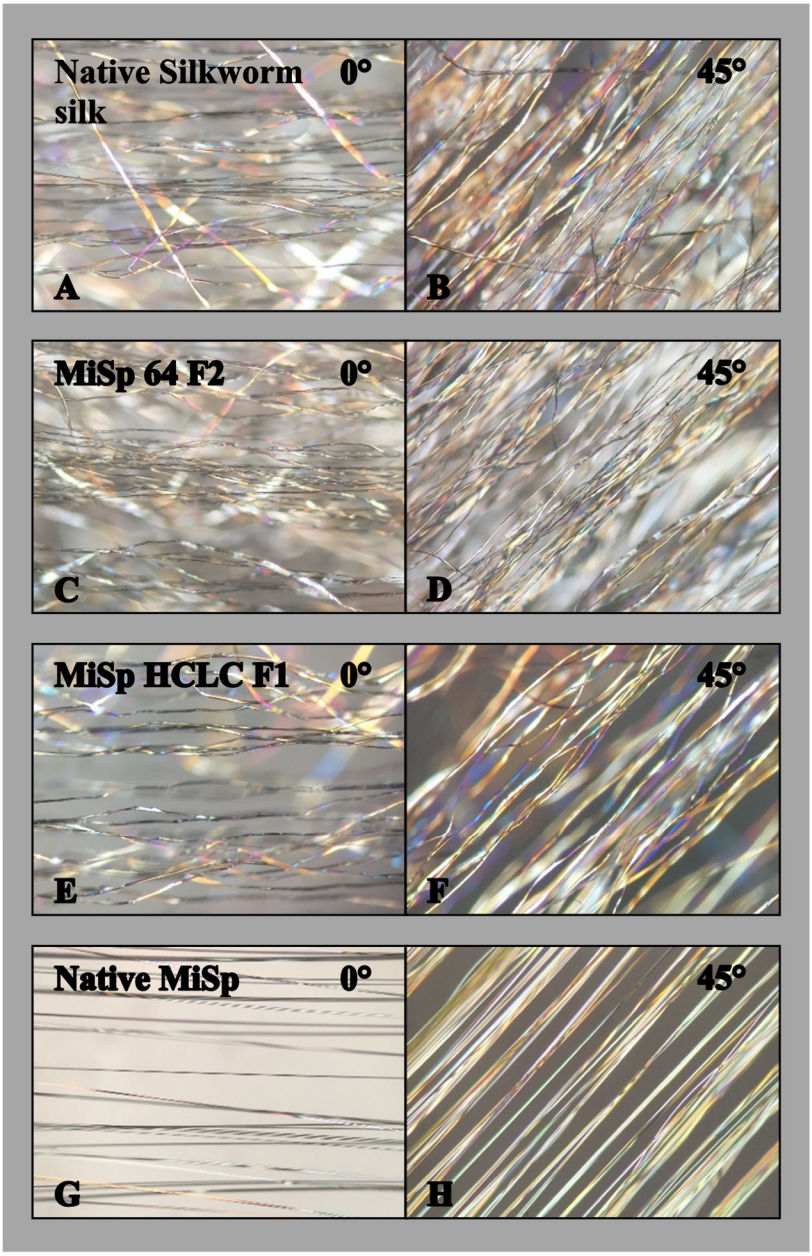

Figure 18. Images of silk bundles under polarized light at 0 degrees and 45 degrees. Highest refringence observed at 45 degrees A and B) Native silkworm silk exhibiting some refringence. C and D) F2 MiSp 64 exhibiting low refringence which results in low fiber properties. E and F) F2 MiSp HL fibers exhibiting high refringence, comparable to native MiSp. G and H) Native MiSp exhibiting highest refringence.

Genomic Analysis

DNA was extracted from the silk moths for PCR to further verify transgenic status of the silkworms. By doing both long-range and regular PCR it was possible to determine which silk moths were transgenic and if any of them were homozygous, meaning if the genetic modification of adding the spider silk gene into the genome was found in both (homozygous) chromosomes or in only one (heterozygous). The first long-range PCR primers covered just outside the LC insert region in the silkworm genome, and covered a section of about 800 bp. If the long-range PCR resulted in PCR products of 12 kb or 14 kb then the silkworm was determined to be transgenic. Figure 19 shows the DNA gels of the long-range PCR of the LC region in the genome. It is difficult to differentiate between 12 kb and 14 kb in the gels since there are only a couple millimeters between the bands marking 10 kb and 20 kb. Lanes 1, 2, 3, 5, 6, 9, 13, 16, 17, and 18 have the correct size bands.

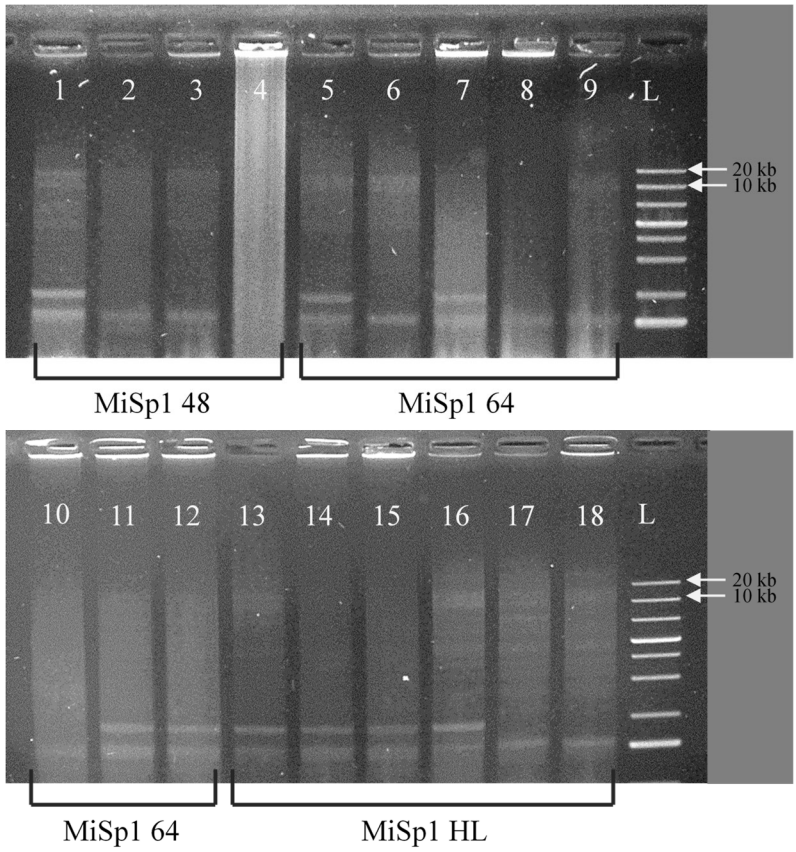

Figure 19. Gel electrophoresis images of long-range PCR product using the LC primers. Lanes with bands just above 10 kb are transgenic. Lanes 1, 2, 3, 5, 6, 9, 13, 16, 17, 18, have the correct size bands.

For the hybrid genomes, a second long-range PCR was necessary to determine if the MiSp1 gene was also present in the HC region of the silkworm genome. The PCR primers covered outside the HC insert region of the silkworm genome. Regular PCR done over the HC insert region would result in a 1.7 kb product if the MiSp1 gene was not present in the HC genome, and long-range PCR would result in a ~14kb product if the MiSp1 gene was present. Figure 20 shows the DNA electrophoresis gels of the long-range PCR of the HC region in the genome, done on the hybrid genomic samples marked 13, 16, 17, and 18 in the long-range LC PCR gel image (Figure 19). Samples 13,

16, and 17 had bands of the correct size, meaning the MiSp1 gene was present in the HC region of the silkworm genome. Sample 18 only showed smearing, possibly due to genome degradation.

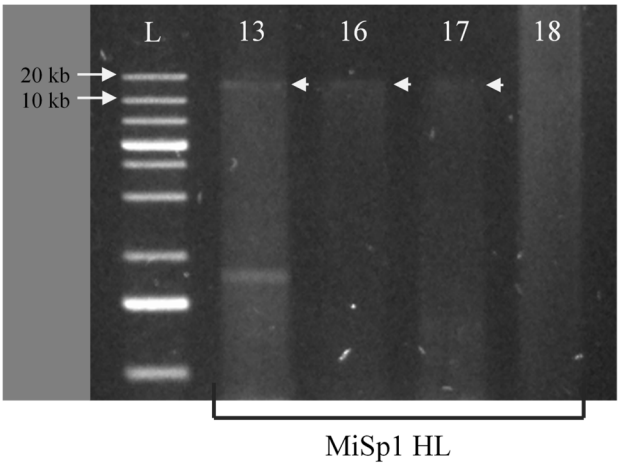

Figure 20. Gel electrophoresis images of long-range PCR product using the HC primers. Lanes with bands just above 10 kb are transgenic. Lanes labeled 13, 16, 17 marked by arrows have the correct size bands.

Regular PCR was conducted following the long-range PCR, only on the verified transgenic samples, to determine if any of them were homozygous for the MiSp1 gene. First, regular PCR was done using the primers covering the LC region of the silkworm genome. PCR products of 800 bp meant the transgenic genome was heterozygous; the long-range PCR product was from the modified allele, while the regular PCR product was from the non-genetically modified allele. If there was no PCR product present in the regular PCR, but where was a long-range PCR product, then the genome was homozygous transgenic. Figure 21 shows the DNA gels of the regular PCR on the LC

insert region of the silkworm genome. Only lanes 1 and 9 had no bands around 800 bp, however it seems the DNA for sample 9 is degraded since there is much more smearing in that lane than for other samples. Only sample 1 from the MiSp1 48 group was verified as homozygous transgenic. None of the remaining samples, apart from the inconclusive sample 9, from the MiSp1 64 or MiSp1 HL group were found to be homozygous.

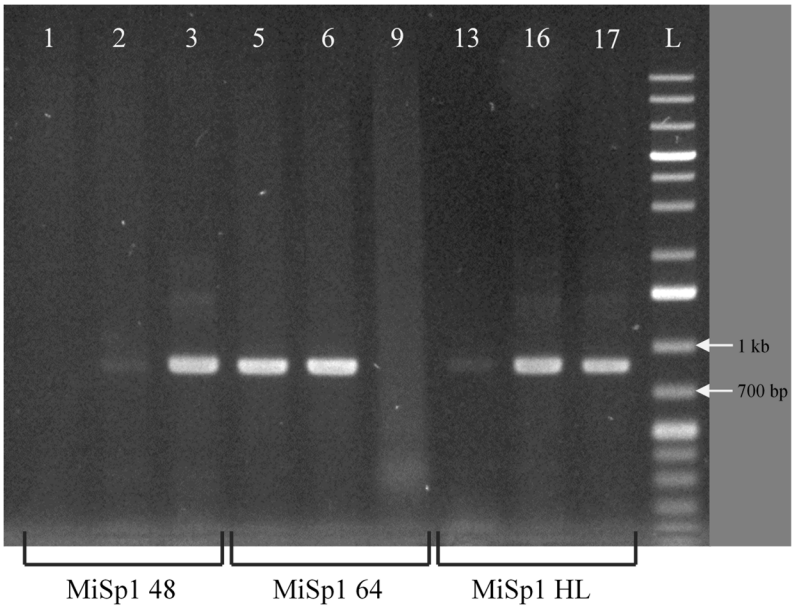

Figure 21. Gel electrophoresis images of DNA product from regular PCR using the LC primers on the silkworm genome. Regular PCR was only performed on verified transgenic genomes from the long-range PCR. Lanes labeled 1 and 9 have no bands around 800 bp, however the DNA is lane 9 appears to be degraded.

Regular PCR was conducted once again using the HC primers, on the hybrid genomes, to determine if any of them were homozygous for the MiSp1 gene in the HC region of the genome. Figure 22 shows a gel electrophoresis image of the PCR products using the HC primers. Samples 13 and 16 are heterozygous. Sample 17 is homozygous,

and sample 18 is inconclusive since there was no band in either the regular PCR and only smearing in the long-range PCR.

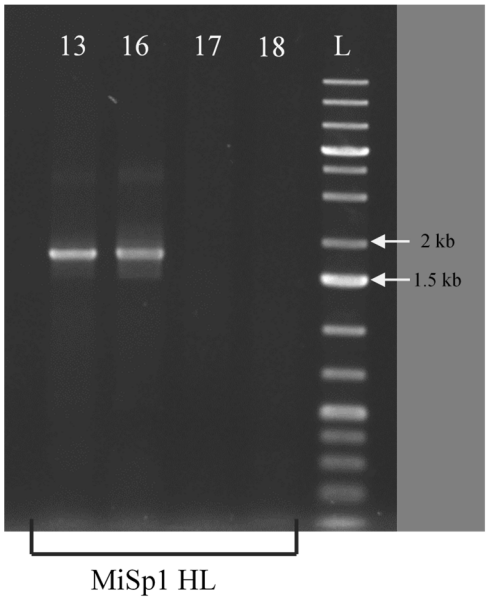

Figure 22. Gel electrophoresis images of DNA product from regular PCR using the HC primers on the silkworm genome. Regular PCR was only performed on verified HC transgenic genomes from the long-range PCR. Lanes labeled 17 and 18 do not have bands around 1.7 kb.

Protein Analysis

Many attempts were done to dissolve the transgenic silk fibers. It was found that the silk is almost impossible to dissolve with any method that still allows for protein characterization. Initially the silk was dissolved in 9M LiSCN to a concentration of 20 µg/µl. SDS-PAGE was conducted with the LiSCN solution as has been performed with normal silkworm silk in the literature.[52–54] but the protein solution would not run evenly

throughout the gel. Coomassie staining showed a lot of smearing, especially towards the top of the gel. Figure 23 shows a picture of the Coomassie stained gel from the LiSCN protein solution.

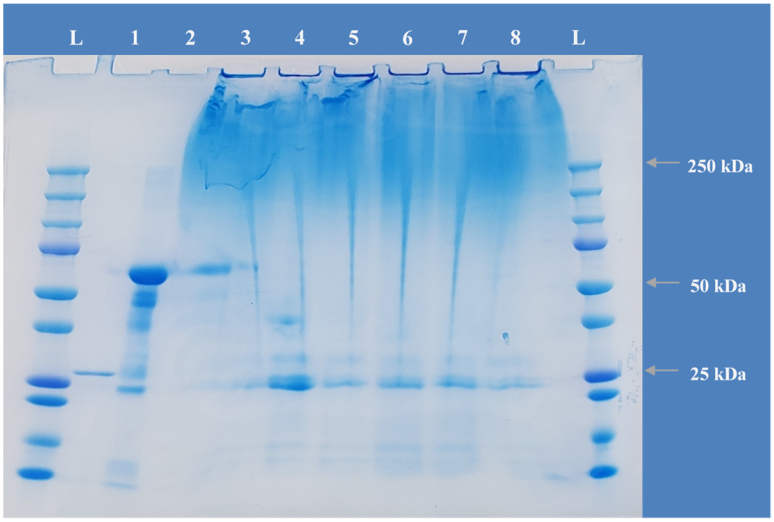

Figure 23. Coomassie stained gel using the 9M LiSCN protein solution. Lane 1) GFP. Lane 2) BSA.

Solutions of HFIP and HFIP + β-mercaptoethanol were also used to attempt to dissolve the silk fibers, but despite making these solutions only 0.25% w/v the silk fibers did not fully dissolve. Similarly, a solution of $CaCl_2$, ethanol, and water was used to attempt to dissolve the silk, but the fibers remained intact. Gland material was collected and dissolved in 8M urea and 8M urea + 2% sarkosyl and used to run another SDS PAGE, however, the gland material gelled after adding the loading buffer and boiling for 5 minutes.

After the previous failed attempts at dissolving the silk, the solution in 9M LiSCN was dialyzed against 50 mm ammonium bicarbonate to reduce the LiSCN concentration in an attempt to reduce the smearing in the gel. The dialyzed solution was collected; however, the silk proteins seemed to aggregate and fall out of solution. The dialyzed solution was then centrifuged, and the supernatant was kept for another SDS PAGE. The remaining pellet from each sample was collected and dissolved in 8M urea and 2% sarkosyl for another SDS PAGE. Figure 24 shows a flow chart summarizing the attempts to dissolve the silk.

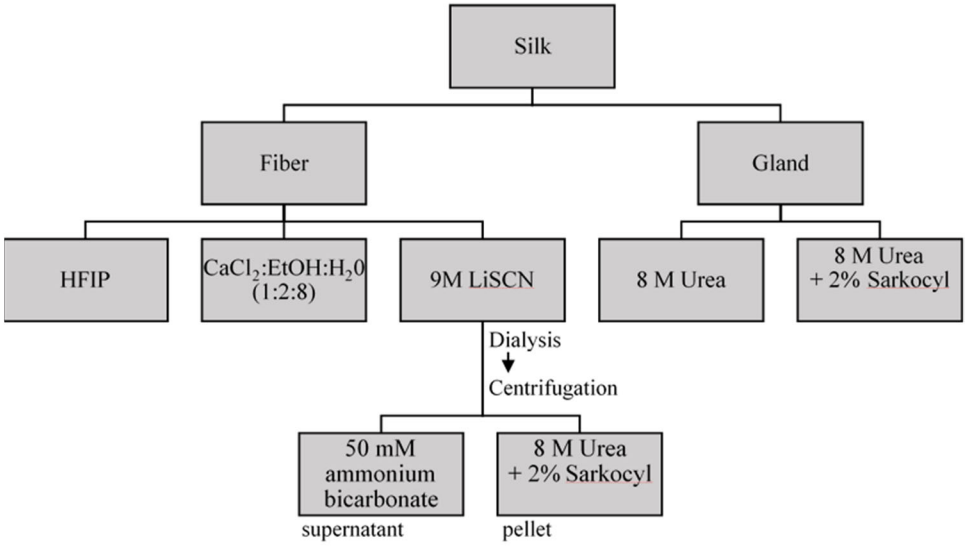

Figure 24. Flow chart outline of all attempts to dissolve the silk from both fiber and gland material.

The concentrations of the dialyzed samples were between 2.3 µg/µl and 10.1 µg/µl for the ammonium bicarbonate solution, and between 0.40 µg/µl and 0.97 µg/µl

for the 8M urea + 2% sarkosyl, measured using a NanoDrop spectrophotometer. The Coomassie stained gels showed that the Ammonium bicarbonate solution only contained low molecular weight proteins, while the 8M urea + 2% sarkosyl solution contained the large molecular weight proteins, and a small amount of the lower molecular weight proteins (25 kDa) but still had a lot of smearing throughout the top part of the gel. The smearing could be due to a combination of several factors, such as protein degradation, overloading the wells, and the MiSp falling out of solution once it is mixed with the loading buffer. Figure 25 shows the Coomassie stained gels from the Ammonium bicarbonate solution and the 8M urea + 2% sarkosyl solution.

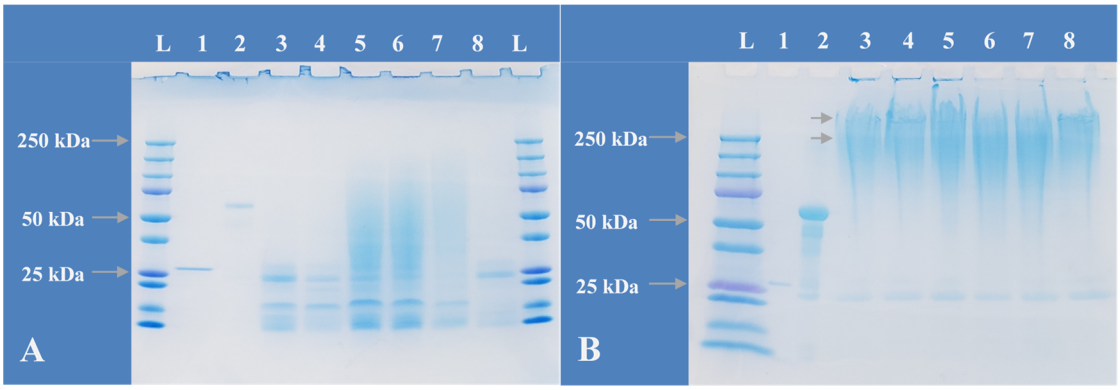

Figure 25. Coomassie stained gels from the 50 mM ammonium bicarbonate solution (A) and the 8M urea + 2% sarkosyl solution (B).

Western blots were also conducted using a GFP antibody, but it was not possible to transfer the large molecular weight proteins onto a membrane (nitrocellulose or PVDF) despite trying different transfer times and different concentrations of methanol in the transfer buffer. Since the transfer of the large proteins onto the membrane proved to

be so difficult, a dot blot was performed instead of a Western blot. Samples from both the 9M LiSCN solution and the 8M urea + 2% sarkosyl solution from the dialyzed pellet were used. The blot using the 8M urea + 2% sarkosyl resulted in positive dots, despite there being some aggregated protein visible in the solution, while the blot 9M LiSCN solution resulted in no positive signal.

It was concluded that the LiSCN interfered with the protein binding onto the membrane, since the samples on the positive blot are from the 8M urea + 2% sarkosyl solutions of the pellet from the dialyzed LiSCN solution. GFP was used as a positive control, while BSA and native silkworm silk were used as negative controls. The dot blot revealed all transgenic silk samples were positive for GFP, verifying the presence of the MiSp1 protein in the silkworm. Figure 26 below shows the dot blot from the dialyzed sample pellet dissolved in 8M urea and 2% sarkosyl.

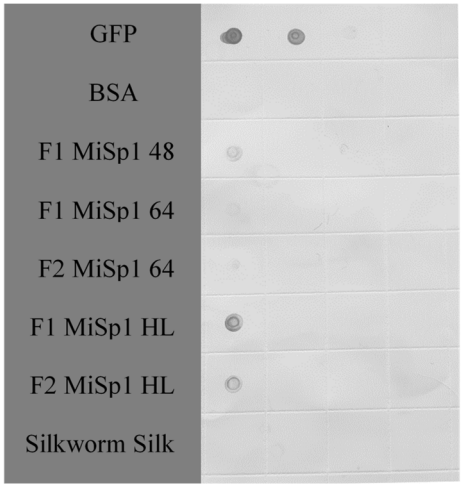

Figure 26. Dot blot from pellet sample after dialyzing the LiSCN solution, centrifuging, and dissolving the pellet in 8M urea and 2% sarkosyl.

A densitometric analysis was then conducted on the dot blot to estimate the concentration of eGFP present in each sample. A standard curve was created from the known concentrations of GFP, and an approximation of spider silk concentration in the dissolved sample was determined from the size ratio of the eGFP (27kDa) to the spider silk protein insert. The MiSp1 48 insert protein size was calculated at 195 kDa, and the MiSp1 64 insert protein size was calculated a 252 kDa, both including the eGFP.

ImageJ was used to analyze an image of the dot blot. An equal sized box was drawn around each of the GFP dots to measure an area intensity of arbitrary units. These area measurements were normalized to a percent concentration based on the known concentration of each dot, with the highest concentration of GFP (200 ng/µl) assigned to 100%, and the next two dots (20 ng/µl and 2 ng/µl of GFP) assigned a proportional percentage based on their area intensity. Table 6 shows the area intensities, percent concentrations, and w/v concentrations of the GFP controls.

Table 6. Normalized percent concentrations of GFP in each control sample calculated from the area intensity of the densitometry analysis.

GFP (ng/ul)	Area intensity	% concentration
2	320.678	2.9
20	6902.376	63.2
200	10919.205	100

Percent concentrations vs. the known concentrations of GFP were then plotted to create a standard curve, and a best fit line was found using the plotted data in Excel. The model equation for the best fit line of the standard curve was found to be

$y = 21.077\ln(x) - 7.7577$, with a fit of $R^2 = 0.9809$. It was not expected to get a linear fit because of the protein saturation limit on the membrane. If the concentration of protein on the membrane is too high, the proteins may stack on top of each other and the antibodies would only bind to the proteins on the surface resulting in a lower estimation of protein quantity. Likewise, the signal intensity of the detection method will also result in a lower estimation of protein quantity if the membrane is overly saturated. In this model "y" is the percent concentration of GFP, with the highest concentration of GFP (200 ng/µl) normalized to 100%, and "x" is the concentration of GFP in ng/µl. Then, the area intensities of the dots from each of the silk samples were measured and converted to percent concentrations and w/v concentrations (ng/ul) based on the 100% concentration of the 200 ng/ul GFP dot. Figure 27 shows the standard curve created from the GFP controls with the calculated concentrations of GFP in each sample.

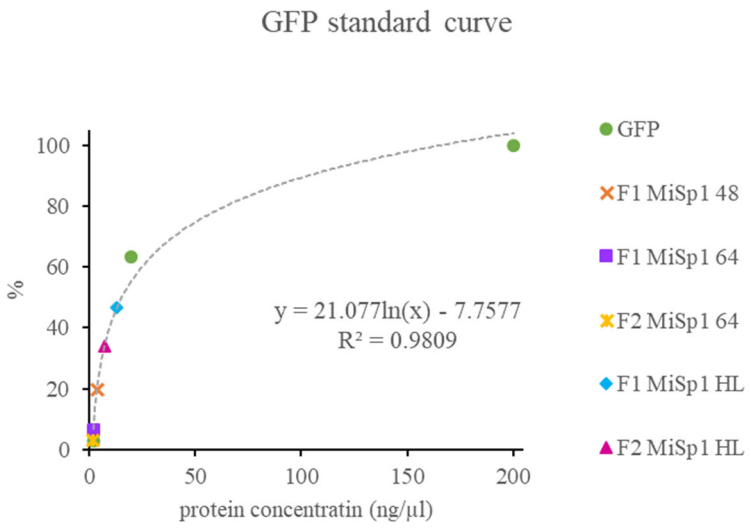

Figure 27. Standard curve calculated from known GFP concentrations, with the calculated GFP concentration from each of the silk samples.

The initial w/v concentrations calculated from the standard curve only account for the eGFP present in each of the silk samples, ignoring the MiSp1 protein that is attached to the eGFP. To fix this issue, a size ratio of the eGFP protein to the MiSp1 48/64 proteins was used to calculate the concentration of dissolved MiSp1. For MiSp1 48 the ratio is 195 kDa/27kDa = 7.2, and for MiSp1 64 the ratio is 252 kDa/27kDa = 9.3. A dissolved spider silk concentration was calculated by multiplying the w/v concentrations of eGFP from the silk samples by the corresponding size ratio of MiSp1 to eGFP. Table 7 shows the area intensity values, percent concentrations, calculated concentrations of eGFP, and the approximate concentrations of dissolved spider silk in each sample.

Table 7. Calculated concentrations of GFP in each sample from the densitometry analysis and estimated concentration of dissolved MiSp1 in each sample.

	Area intensity	**Percent concentration**	**GFP (ng/µl)**	**MiSp1 (ng/µl)**
MiSp 48 F1	2174.012	19.9	3.7	26.4
MiSp 64 F1	707.577	6.5	2.0	14.0
MiSp 64 F2	340.385	3.1	1.7	15.6
MiSp HC F1	5095.062	46.6	13.2	123.0
MiSp HC F2	3707.305	34.0	7.2	67.3

Despite these calculations, finding the percent spider silk content in the whole fiber is not currently possible since much of the protein remained insoluble in the urea solution. Further ideas to dissolve the transgenic silk fibers and calculate their spider silk content are discussed in the Future Work section.

CONCLUSIONS

Summary and Conclusions

As stated in the introduction, the goals of this project were to incorporate MiSp1 into the light chain region of the silkworm genome (MiSp1 in the LC) by using a CRISPR/Cas 9 system; crossbreed transgenic silkworms containing MiSp1 in the LC with a previously made transgenic line containing the MiSp1 protein in the heavy chain (MiSp1 in the HC) to make a hybrid line which has the MiSp1 protein in both the HC and the LC (MiSp1 HL); confirm increase in mechanical properties through tensile testing; validate the presence of the MiSp1 gene in the silkworm genome; and verify the presence of the MiSp1 protein in the silkworm fiber. It was hypothesized that the introduction of MiSp1 into the light chain region of the silkworm silk would result in a fiber with a decrease in maximum strain and an increase in tensile strength when compared to native silkworm silk.

After genetically modifying the silkworms, the expression of full-length MiSp1 protein and its incorporation into the silk fiber was verified through a combination of the following methods:

- Visual fluorescence of transgenic silkworm cocoons
- Improved mechanical properties (in a predictable fashion)
- PCR analysis of transgenic genomes
- SDS-PAGE and dot blot

The first visual proof of transgenesis was observed once the completed cocoons were placed under a UV light causing the GFP reporter protein to glow which was especially important for quick identification of transgenic cocoons, as well as breeding the next generation of silkworms.

The results of tensile testing showed no statistically significant differences in the mechanical properties of the F1 generation of transgenic silkworms compared to the native silkworm silk, while the F2 generation groups had both the highest and lowest mechanical properties. The F2 MiSp1 64, the group of sick silkworms, had the silk with the lowest mechanical properties of all the groups including the native silkworm group, and the F2 MiSp HL group had the silk with the highest mechanical properties which only had a 100 MPa difference in maximum average stress than the native MiSp group.

It was also found that the average maximum strain of the silk was not affected by the MiSp1 insert, as was initially hypothesized, with all the transgenic silk groups having over double the maximum strain of the native MiSp silk. Due to the unexpected high strain of the transgenic silk combined with the expected increase in the strength of the fibers, all groups had higher energy to break values than the native MiSp including the F2 MiSp1 64 group. However, in terms of elastic modulus, the native MiSp still had the highest value, with the F2 MiSp1 HL group approaching the native MiSp group. All other groups, apart from the F2 MiSp1 64 group, saw an increase in elastic modulus compared to the native silkworm silk group.

It was hypothesized that the low properties of the F2 MiSp 64 group were due to the silkworms' inability to spin the fibers with proper stretch, to align the crystalline structures and achieve high mechanical properties. Since the crystalline structures could

not be directly observed, the birefringent property of silk was used to get a relative idea of the crystalline orientation in each silk group. The refringence of the silk groups at different angles was observed with polarized light microscopy, with the most dramatic changes in refringence between orientations, attributed to the highest orientation of crystalline structures. It was found that the F2 MiSp1 64 had the least observed change in refringence when compared to other groups which is consistent with the mechanical properties of the silk, while the F2 MiSp1 HL group had the most marked change in refringence and similar to the change in refringence of the native MiSp group.

A DNA analysis was conducted by PCR of the silkworm genome surrounding the insert regions. Long-range PCR was used to make PCR products of the MiSp1 insert, while regular PCR was used to make products of the insert region. The results of the two types of PCR were combined to determine transgenicity of the genomes, and whether the transgenic genomes were homozygous or heterozygous.

Of the 18 genomes collected, only 10 were determined to be transgenic for MiSp1 in the LC, and only 3 of the 6 possible HL hybrids had both the MiSp1 gene in the HC and the LC. Only one of the genomes of the MiSp1 in the LC was found to be homozygous, and one of the HL samples was found be homozygous for the MiSp in the HC. Knowing if the MiSp1 gene is present in one or both alleles is important when breeding the moths for the next generations of silkworms to increase the number of transgenic silkworms and the amount of spider silk they can produce. This knowledge becomes even more important for breeding the hybrid transgenic silkworms which contain the MiSp genes in both the HC and LC region of the genome and can result in various combination of single transgenic or hybrid transgenic offspring.

A protein analysis was conducted in an effort to determine the percent of spider silk present in the transgenic silkworm silk. Many obstacles were encountered, first to dissolve the silk, then to run SDS-PAGE, and finally to transfer the protein from a gel onto a membrane for Western blotting. The solutions used to dissolve the silk interfered with the protein running smoothly through the gel during SDS-PAGE or only kept small proteins in solution; the most successful gels still resulted in some smearing; and transfer of the large proteins onto a membrane was never successful. However, the inability to fully dissolve the silk suggests the silk is highly durability, even in applications with potentially corrosive environments.

Due to all the problems encountered trying transfer the protein onto a membrane after SDS-PAGE, a dot blot was used instead of a Western blot. The dot blot showed eGFP present in all the transgenic samples with the most GFP present in the F1 MiSp1 HL group. A densitometry analysis of the dot blot was conducted to determine the quantity of eGFP present in each sample based on known concentration of pure GFP, which served as a positive control, and then calculate the amount of spider silk present based on the size ratio of eGFP to the MiSp1 inserts. While the densitometry analysis was only semi-quantitative, it is a beginning step towards protein characterization and quantification in the transgenic silk.

Future Work

There are many ways in which this project could evolve, whether it is further

manipulating the properties of silk, finding improved methods of characterization, or developing new applications for the transgenic silk. The following paragraphs discuss a few ideas for future directions to take this project.

While two different size inserts were used to make the transgenic worms, there was only one generation to compare the mechanical properties of the resulting silk. Studies to optimize the mechanical properties of the transgenic silk in more generations could be conducted with transgenic silkworms containing different sizes of the spider silk. Likewise, the stability of the spider silk insert in the genome could be observed through several generations.

This project was the first to cross-breed silkworms from two different transgenic lines to create a hybrid with both the MiSp1 in the HC and LC. The silk from these hybrid groups was improved from the single transgenic LC samples, and even began to approach the mechanical properties of native MiSp. This same concept can be used to create hybrid silkworms with other types of spider silk, such as MaSp1 to further increase the mechanical properties of transgenic silk.

For more accurate results in terms of protein size and quantification of total MiSp in the silk, more work needs to be done to find ways to dissolve the transgenic silk in solutions that allow for better SDS-PAGE and Western blotting. The solutions used in this project to dissolve the silk were either too chaotropic to use in protein detection methods or did not fully dissolve the silk. It would be interesting to do step-wise dialysis using larger volumes of dissolved silk to slowly lower the concentration of the solution used to dissolve the silk (such as LISCN) and help prevent the dissolved silk from precipitating. Other methods, such as FTIR or XRD which do not require a dissolved

fiber, could also be used to quantify the MiSp1 in the silk fiber based on the quantity of crystalline structures.

Finally, since this project focused on the development of transgenic silk, it is important to look towards the future of transgenic silk as a biomaterial and its possible applications in industry. By combining different types of spider silk into silkworm silk through genetic engineering and cross-breeding, it would be possible to tailor the transgenic silk to suit a broad array of needs in different industries, while also being a more sustainable biomaterial. Potential industries for transgenic silk could range from medical applications, to the textile industry, or even material's applications to add strength or extensibility to other materials.

Engineering Significance

It is the goal of any engineer to design products or processes which will have a positive impact to their community. This is accomplished through a cycle of designing, testing, implementing, and evaluating until the product/process has met the required specifications. This design process can be used at large and small scales within every aspect of a project with the purpose of creating improvement in products and processes, while also meeting the needs of industries.

The main goal of this project was to create a transgenic silk fiber which increased mechanical properties by inserting an MiSp1 gene into the LC region of the silkworm silk genome. Two sizes of spider silk genes (MiSp1 48 and MiSp1 64) were

used in case one was too big to be efficiently introduced into the silkworm genome. The resulting transgenic silk from the both MiSp1 gene sizes had an increase in average maximum strength of 120-130 MPa in the first generation compared to native silkworm silk, but there was no significant difference in the mechanical strength increase between the MiSp1 64 and 48 groups. It was not possible however, to determine if one of the inserts was more stable than the other, since there was only one generation to compare.

To further increase the mechanical properties of the silk, the transgenic moths from this project were bred with a transgenic line of moths which contained the MiSp1 gene in the HC region of the silkworm region, potentially doubling the amount of spider silk present in the transgenic silk. Within two generations, this hybrid line resulted in transgenic silk with a significantly higher toughness than the native MiSp, or the native silkworm silk, through the combination of the maximum stress approaching that of native MiSp and the maximum strain of silkworm silk.

While the spider silk gene insert alone would lead to increased mechanical properties, the eGFP gene was added before the MiSp1 gene to serve as a reporter gene and dramatically reduce the time required to identify transgenic cocoons from non-transgenic cocoons. Without the eGFP, genomic or amino acid analyses would be necessary to determine transgenicity for each silkworm/cocoon, which are both expensive, time consuming, and would potentially disrupt the silk production cycles, especially at an industrial scale.

Several methods were used to dissolve the silk for Western blotting. The solution used had to dissolve the silk and keep it in solution while allowing for band resolution in the SDS-PAGE. In all cases, the silk would either not dissolve, or result in an uneven

and smeared SDS-PAGE with low band resolution. The process for dissolution was improved by adding a dialysis step after dissolving in LiSCN and re-dissolving the precipitate in urea and sarkosyl. The procedure to transfer the large proteins from the gel onto a membrane for Western blotting was also optimized by changing the transfer buffer, voltage, temperature, and time. The most effective transfer was done with a transfer buffer containing 10% methanol, overnight at 4°C and 40V, with an additional hour at 100V at the end. The results of the Western blot were negative, however, the Coomassie stained gel from the transfer showed the large molecular weight proteins still in the gel. Ultimately, a dot blot was done to avoid the problems in the transfer from the gel onto a membrane, although the molecular weight of the MiSp1 inserts could not be verified.

The many failed attempts at fiber dissolution highlight the durability of the transgenic silk, a property that is desirable in a material that is primarily used in textile applications[38,55]. While this durability proved problematic in quantifying the amount of MiSp1 present in the silk, it is ultimately a positive property, especially in applications where there is need for a strong and durable material.

Spider silk as a biomaterial has long been studied, with the goal of harnessing this strong biomaterial for large scale production. This project has shown it is possible to genetically modify silkworms to produce a fiber with similar mechanical properties to native MiSp and serves as a background for optimization and scale-up of a durable biomaterial. Considerations for scale up to an industrial level are involved at every step, from the genetic modification, to consistency in the quality of the silk. Before genetically modified silkworm silk can be commercially available, it is necessary to

make sure the spider silk gene addition is stable within the genome for several generations, to avoid the high cost and decrease in transgenic silkworm yields involved with genetically modifying each new generation of silkworms.

Next the sericulture process needs to become more regulated, to maintain the same quality of silk across silk farming location and through silkworm generations. Sericulture regulation would involve creating set protocols to describe ways to help structure the sericulture process and control the quality of silk more closely. These protocols should consider:

- Environmental conditions such as temperature and humidity
- Type and preparation of synthetic chow or natural food fed
- Separation of silkworms at different larval stages
- Conditions for silkworms to spin cocoons
- Cocoon harvesting, degumming, and unwinding.
- Additional silk processing

Further, quality control testing should be done regularly, especially at an industrial scale, even once the sericulture process is more regulated. DNA, protein, and mechanical analyses could be done to randomly selected batches of silkworms and their silk to ensure the quality of the silk is consistent and meets industrial requirements.

Finally, the genetic engineering work in this project validates the production of synthetic spider silk in an established organism and industry. The results of this project demonstrated that the properties of silkworm silk can be predictably altered through genetic engineering and help advance the large scale production of spider silk as a commercial biomaterial.

APPENDIX

IMAGE PERMISSIONS

Image permission for Figure 1.

SPRINGER NATURE LICENSE
TERMS AND CONDITIONS

Apr 25, 2019

This Agreement between Ana Laura Licon ("You") and Springer Nature ("Springer Nature") consists of your license details and the terms and conditions provided by Springer Nature and Copyright Clearance Center.

License Number	4576080602043
License date	Apr 25, 2019
Licensed Content Publisher	Springer Nature
Licensed Content Publication	Nature Chemical Biology
Licensed Content Title	Toward spinning artificial spider silk
Licensed Content Author	Anna Rising, Jan Johansson
Licensed Content Date	Apr 17, 2015
Licensed Content Volume	11
Licensed Content Issue	5
Type of Use	Thesis/Dissertation
Requestor type	academic/university or research institute
Format	print and electronic
Portion	figures/tables/illustrations
Number of figures/tables/illustrations	1
High-res required	no
Will you be translating?	no
Circulation/distribution	<501
Author of this Springer Nature content	no
Title	SpiderWorms: Using Silkworms as Hosts to Produce a Hybrid Silkworm-Spider Silk Fiber
Institution name	Utah State University
Expected presentation date	Aug 2019
Order reference number	1
Portions	Figure 1a. Image of the different types of spider silk.
Requestor Location	Ana Laura Licon 320 E 2475 N LOGAN, UT 84341 United States Attn: Ana Laura Licon
Total	0.00 USD

Image Permission for Figure 3.

Int. J. Mol. Sci. **2016**, *17*(8), 1290; https://doi.org/10.3390/ijms17081290 Open Access Review

Silk Spinning in Silkworms and Spiders

Marlene Andersson [1], **Jan Johansson** [1,2] and **Anna Rising** [1,2,*]

[1] Department of Anatomy, Physiology and Biochemistry, Swedish University of Agricultural Sciences, Uppsala 75651, Sweden

[2] Department of Neurobiology, Care Sciences and Society (NVS), Karolinska Institutet, Stockholm 14157, Sweden

* Author to whom correspondence should be addressed.

Academic Editors: John G. Hardy and Chris Holland

Received: 17 June 2016 / Revised: 31 July 2016 / Accepted: 2 August 2016 / Published: 9 August 2016

(This article belongs to the Special Issue Silk-Based Materials: From Production to Characterization)

Full-Text | PDF [3298 KB, uploaded 9 August 2016] | Figures

Abstract

Spiders and silkworms spin silks that outcompete the toughness of all natural and manmade fibers. Herein, we compare and contrast the spinning of silk in silkworms and spiders, with the aim of identifying features that are important for fiber formation. Although spiders and silkworms are very distantly related, some features of spinning silk seem to be universal. Both spiders and silkworms produce large silk proteins that are highly repetitive and extremely soluble at high pH, likely due to the globular terminal domains that flank an intermediate repetitive region. The silk proteins are produced and stored at a very high concentration in glands, and then transported along a narrowing tube in which they change conformation in response primarily to a pH gradient generated by carbonic anhydrase and proton pumps, as well as to ions and shear forces. The silk proteins thereby convert from random coil and alpha helical soluble conformations to beta sheet fibers. We suggest that factors that need to be optimized for successful production of artificial silk proteins capable of forming tough fibers include protein solubility, pH sensitivity, and preservation of natively folded proteins throughout the purification and initial spinning processes. View Full-Text

Keywords: spidroin; fibroin; *Bombyx mori*; major ampullate gland; carbonic anhydrase; pH gradient; protein conformation

► **Figures**

Image Permission for Figure 5.

Review Order

Please review the order details and the associated terms and conditions.

No royalties will be charged for this reuse request although you are required to obtain a license and comply with the license terms and conditions. To obtain the license, click the Accept button below.

Licensed Content Publisher	Springer Nature
Licensed Content Publication	Nature Protocols
Licensed Content Title	Genome engineering using the CRISPR-Cas9 system
Licensed Content Author	F Ann Ran, Patrick D Hsu, Jason Wright, Vineeta Agarwala, David A Scott et al.
Licensed Content Date	Oct 24, 2013
Licensed Content Volume	8
Licensed Content Issue	11
Type of Use	Thesis/Dissertation
Requestor type	academic/university or research institute
Format	print and electronic
Portion	figures/tables/illustrations
Number of figures/tables/illustrations	1
High-res required	no
Will you be translating?	no
Circulation/distribution	<501
Author of this Springer Nature content	no
Title	SpiderWorms: Using Silkworms as Hosts to Produce a Hybrid Silkworm-Spider Silk Fiber
Institution name	Utah State University
Expected presentation date	Aug 2019
Order reference number	5
Portions	Figure 2. Depiction of CRISPR/Cas9 system and repair mechanisms.
Requestor Location	Ana Laura Licon 320 E 2475 N LOGAN, UT 84341 United States Attn: Ana Laura Licon
Total	0.00 USD

REFERENCES

(1) Morgan, E. Gossamer Days: Spiders, Humans and Their Threads (Strange Attractor Press, **2016**)

(2) Lewis, R. Unraveling the Weave of Spider Silk. *BioScience* **1996**, *46* (9), 636–638.

(3) A Golden Spider-Silk Textile. *The Art Institute of Chicago* Available at: https://www.artic.edu/exhibitions/3280/a-golden-spider-silk-textile

(4) Rising, A.; Johansson, J. Toward Spinning Artificial Spider Silk. *Nature Chemical Biology* **2015**, *11* (5), 309–315.

(5) Tokareva, O.; Michalczechen-Lacerda, V. A.; Rech, E. L.; Kaplan, D. L. Recombinant DNA Production of Spider Silk Proteins. *Microb Biotechnol* **2013**, *6* (6), 651–663.

(6) Colgin, M. A.; Lewis, R. V. Spider Minor Ampullate Silk Proteins Contain New Repetitive Sequences and Highly Conserved Non-Silk-like "Spacer Regions." *Protein Sci.* **1998**, *7* (3), 667–672.

(7) Lewis, R. V. Spider Silk: Ancient Ideas for New Biomaterials. *Chem. Rev.* **2006**, *106* (9), 3762–3774.

(8) Römer, L.; Scheibel, T. The Elaborate Structure of Spider Silk. *Prion* **2008**, *2* (4), 154–161.

(9) Xu, M.; Lewis, R. V. Structure of a Protein Superfiber: Spider Dragline Silk. *Proc. Natl. Acad. Sci. U S A* **1990**, *87* (18), 7120–7124.

(10) Gosline, J. M. The Mechanical Design of Spider Silks: From Fibroin Sequence to Mechanical Function. *J. Exp. Biol*. **1999**, 202 (9), 3295-3303.

(11) Fahnestock, S. R.; Irwin, S. L. Synthetic Spider Dragline Silk Proteins and Their Production in Escherichia Coli. *Applied Microbiology and Biotechnology* **1997**, *47* (1), 23–32.

(12) Adrianos, S. L.; Teulé, F.; Hinman, M. B.; Jones, J. A.; Weber, W. S.; Yarger, J. L.; Lewis, R. V. Nephila Clavipes Flagelliform Silk-Like GGX Motifs Contribute to Extensibility and Spacer Motifs Contribute to Strength in Synthetic Spider Silk Fibers. *Biomacromolecules* **2013**, *14* (6), 1751–1760.

(13) Opell, B. D.; Hendricks, M. L. The Role of Granules within Viscous Capture Threads of Orb-Weaving Spiders. *Journal of Experimental Biology* **2010**, *213* (2), 339–346.

(14) Xia, X.-X.; Qian, Z.-G.; Ki, C. S.; Park, Y. H.; Kaplan, D. L.; Lee, S. Y. Native-Sized Recombinant Spider Silk Protein Produced in Metabolically Engineered Escherichia Coli Results in a Strong Fiber. *Proc. Natl. Acad. Sci. U S A* **2010**, *107* (32), 14059–14063.

(15) Hayashi, C. Y.; Shipley, N. H.; Lewis, R. V. Hypotheses That Correlate the Sequence, Structure, and Mechanical Properties of Spider Silk Proteins. *Int. J. Biol. Macromol.* **1999**, *24* (2–3), 271–275.

(16) Tatham, A. S.; Shewry, P. R. Elastomeric Proteins: Biological Roles, Structures and Mechanisms. *Trends in Biochemical Sciences* **2000**, *25* (11), 567–571.

(17) Holland, G. P.; Jenkins, J. E.; Creager, M. S.; Lewis, R. V.; Yarger, J. L. Solid-State NMR Investigation of Major and Minor Ampullate Spider Silk in the Native and Hydrated States. *Biomacromolecules* **2008**, *9* (2), 651–657.

(18) Chen, G.; Liu, X.; Zhang, Y.; Lin, S.; Yang, Z.; Johansson, J.; Rising, A.; Meng, Q. Full-Length Minor Ampullate Spidroin Gene Sequence. *PLoS ONE* **2012**, *7* (12), e52293.
(19) Yamaguchi, K.; Kikuchi, Y.; Takagi, T.; Kikuchi, A.; Oyama, F.; Shimura, K.; Mizuno, S. Primary Structure of the Silk Fibroin Light Chain Determined by CDNA Sequencing and Peptide Analysis. *Journal of Molecular Biology* **1989**, *210* (1), 127–139. https:
(20) Breslauer, D. N.; Lee, L. P.; Muller, S. J. Simulation of Flow in the Silk Gland. *Biomacromolecules* **2009**, *10* (1), 49–57.
(21) Hinman, M. B.; Jones, J. A.; Lewis, R. V. Synthetic Spider Silk: A Modular Fiber. *Trends in Biotechnology* **2000**, *18* (9), 374–379.
(22) Prince, J. T.; McGrath, K. P.; DiGirolamo, C. M.; Kaplan, D. L. Construction, Cloning, and Expression of Synthetic Genes Encoding Spider Dragline Silk. *Biochemistry* **1995**, *34* (34), 10879–10885.
(23) Brooks, A. E.; Nelson, S. R.; Jones, J. A.; Koenig, C.; Hinman, M.; Stricker, S.; Lewis, R. V. Distinct Contributions of Model MaSp1 and MaSp2 like Peptides to the Mechanical Properties of Synthetic Major Ampullate Silk Fibers as Revealed in Silico. *Nanotechnol Sci Appl* **2008**, *1*, 9–16.
(24) Koeppel, A.; Holland, C. Progress and Trends in Artificial Silk Spinning: A Systematic Review. *ACS Biomater. Sci. Eng.* **2017**, *3* (3), 226–237.
(25) Vollrath, F.; Madsen, B.; Shao, Z. The Effect of Spinning Conditions on the Mechanics of a Spider's Dragline Silk. *Proc Biol Sci* **2001**, *268* (1483), 2339–2346.
(26) Lazaris, A.; Arcidiacono, S.; Huang, Y.; Zhou, J.-F.; Duguay, F.; Chretien, N.; Welsh, E. A.; Soares, J. W.; Karatzas, C. N. Spider Silk Fibers Spun from Soluble Recombinant Silk Produced in Mammalian Cells. *Science* **2002**, *295* (5554), 472–476.
(27) Albertson, A. E.; Teulé, F.; Weber, W.; Yarger, J. L.; Lewis, R. V. Effects of Different Post-Spin Stretching Conditions on the Mechanical Properties of Synthetic Spider Silk Fibers. *Journal of the Mechanical Behavior of Biomedical Materials* **2014**, *29*, 225–234.
(28) Copeland, C. G.; Bell, B. E.; Christensen, C. D.; Lewis, R. V. Development of a Process for the Spinning of Synthetic Spider Silk. *ACS Biomaterials Science & Engineering* **2015**.
(29) Jones, J. A.; Harris, T. I.; Tucker, C. L.; Berg, K. R.; Christy, S. Y.; Day, B. A.; Gaztambide, D. A.; Needham, N. J. C.; Ruben, A. L.; Oliveira, P. F.; et al. More Than Just Fibers: An Aqueous Method for the Production of Innovative Recombinant Spider Silk Protein Materials. *Biomacromolecules* **2015**, *16* (4), 1418–1425.
(30) Kato, T.; Kajikawa, M.; Maenaka, K.; Park, E. Y. Silkworm Expression System as a Platform Technology in Life Science. *Appl Microbiol Biotechnol* **2010**, *85* (3), 459–470.
(31) Barber, E. J. W. *Prehistoric Textiles: The Development of Cloth in the Neolithic and Bronze Ages with Special Reference to the Aegean*; Princeton University Press, **1991**.
(32) Murugesh Babu K. "Silk From Silkworms as High Performance Fibers" In

Structure and Properties of High-Performance Fibers; Elsevier, 2017.
(33) Pérez-Rigueiro, J.; Elices, M.; Llorca, J.; Viney, C. Effect of Degumming on the Tensile Properties of Silkworm (Bombyx Mori) Silk Fiber. *Journal of Applied Polymer Science 84* (7), 1431–1437.
(34) Inoue, S.; Tanaka, K.; Arisaka, F.; Kimura, S.; Ohtomo, K.; Mizuno, S. Silk Fibroin of Bombyx Mori Is Secreted, Assembling a High Molecular Mass Elementary Unit Consisting of H-Chain, L-Chain, and P25, with a 6:6:1 Molar Ratio. *J. Biol. Chem.* **2000**, *275* (51), 40517–40528.
(35) Sehnal, F.; Žurovec, M. Construction of Silk Fiber Core in Lepidoptera. *Biomacromolecules* **2004**, *5* (3), 666–674.
(36) Malay, A. D.; Sato, R.; Yazawa, K.; Watanabe, H.; Ifuku, N.; Masunaga, H.; Hikima, T.; Guan, J.; Mandal, B. B.; Damrongsakkul, S.; et al. Relationships between Physical Properties and Sequence in Silkworm Silks. *Scientific Reports* **2016**, *6*, 27573.
(37) Craig, C. L.; Riekel, C. Comparative Architecture of Silks, Fibrous Proteins and Their Encoding Genes in Insects and Spiders. *Comparative Biochemistry and Physiology Part B: Biochemistry and Molecular Biology* **2002**, *133* (4), 493–507.
(38) Koh, L.-D.; Cheng, Y.; Teng, C.-P.; Khin, Y.-W.; Loh, X.-J.; Tee, S.-Y.; Low, M.; Ye, E.; Yu, H.-D.; Zhang, Y.-W.; et al. Structures, Mechanical Properties and Applications of Silk Fibroin Materials. *Progress in Polymer Science* **2015**, *46*, 86–110.
(39) Zafar, M. S.; Belton, D. J.; Hanby, B.; Kaplan, D. L.; Perry, C. C. Functional Material Features of Bombyx Mori Silk Light vs. Heavy Chain Proteins. *Biomacromolecules* **2015**, *16* (2), 606–614.
(40) Andersson, M.; Johansson, J.; Rising, A. Silk Spinning in Silkworms and Spiders. *Int J Mol Sci* **2016**, *17* (8).
(41) Omenetto, F. G.; Kaplan, D. L. New Opportunities for an Ancient Material. *Science* **2010**, *329* (5991), 528–531.
(42) Hilbrant, M.; Damen, W. G. M. The Embryonic Origin of the Ampullate Silk Glands of the Spider Cupiennius Salei. *Arthropod Structure & Development* **2015**, *44* (3), 280–288.
(43) Andersson, M.; Holm, L.; Ridderstråle, Y.; Johansson, J.; Rising, A. Morphology and Composition of the Spider Major Ampullate Gland and Dragline Silk. *Biomacromolecules* **2013**, *14* (8), 2945–2952.
(44) Asakura, T.; Umemura, K.; Nakazawa, Y.; Hirose, H.; Higham, J.; Knight, D. Some Observations on the Structure and Function of the Spinning Apparatus in the Silkworm Bombyx Mori. *Biomacromolecules* **2007**, *8* (1), 175–181.
(45) Askarieh, G.; Hedhammar, M.; Nordling, K.; Saenz, A.; Casals, C.; Rising, A.; Johansson, J.; Knight, S. D. Self-Assembly of Spider Silk Proteins Is Controlled by a PH-Sensitive Relay. *Nature* **2010**, *465* (7295), 236–238.
(46) Domigan, L. J.; Andersson, M.; Alberti, K. A.; Chesler, M.; Xu, Q.; Johansson, J.; Rising, A.; Kaplan, D. L. Carbonic Anhydrase Generates a PH Gradient in Bombyx Mori Silk Glands. *Insect Biochemistry and Molecular Biology* **2015**, *65*, 100–106.
(47) Teulé, F.; Miao, Y.-G.; Sohn, B.-H.; Kim, Y.-S.; Hull, J. J.; Fraser, M. J.; Lewis, R. V.; Jarvis, D. L. Silkworms Transformed with Chimeric Silkworm/Spider Silk

Genes Spin Composite Silk Fibers with Improved Mechanical Properties. *PNAS* **2012**, *109* (3), 923–928.

(48) Zhang, X.; Day, B.; Harris, T.; Oliveira, P.; Knittel, C.; Licon, A. L.; Gong, C.; Dion, G.; Lewis, R. V.; Jones, J. A. CRISPR/Cas9 Initiated Transgenic Silkworms as a Natural Spinner for Spider Silk. *Biomacromolecules* **2019**.

(49) Ran, F. A.; Hsu, P. D.; Wright, J.; Agarwala, V.; Scott, D. A.; Zhang, F. Genome Engineering Using the CRISPR-Cas9 System. *Nature Protocols* **2013**, *8* (11), 2281–2308.

(50) Lefèvre, T.; Rousseau, M.-E.; Pézolet, M. Protein Secondary Structure and Orientation in Silk as Revealed by Raman Spectromicroscopy. *Biophysical Journal* **2007**, *92* (8), 2885–2895.

(51) Johnson, S. A. Silkworms; *First Avenue Editions*, **1989**.

(52) TAKASU, Y.; YAMADA, H.; TSUBOUCHI, K. Isolation of Three Main Sericin Components from the Cocoon of the Silkworm, Bombyx Mori. *Bioscience, Biotechnology, and Biochemistry* **2002**, *66* (12), 2715–2718.

(53) Sponner, A.; Vater, W.; Monajembashi, S.; Unger, E.; Grosse, F.; Weisshart, K. Composition and Hierarchical Organisation of a Spider Silk. *PLOS ONE* **2007**, *2* (10), e998.

(54) Schoeser, M. Silk; *Yale University Press,* **2007**.

(55) Reddy, R. M. Innovative and Multidirectional Applications of Natural Fibre, Silk - A Review. *J. Entomol*, **2009**. 2 (5), 71-75.